AEAT/R/ENV/0355 Issue 1

The Temporal Dependence of Ozone Precursor Emissions: Estimation and Application

Report on the contracts EPG 1/3/134 and EPG 1/3/143

Michael E. Jenkin, Timothy P. Murrells and Neil R. Passant

November 2000

AEAT/R/ENV/0355 Issue 1

The Temporal Dependence of Ozone Precursor Emissions: Estimation and Application

Report on the contracts EPG 1/3/134 and EPG 1/3/143

Michael E. Jenkin, Timothy P. Murrells and Neil R. Passant

November 2000

Title	The Temporal Dependence of Ozone Precursor Emissions
Customer	DETR, AEQ Division,
Customer reference	EPG 1/3/143; EPG 1/3/134
Confidentiality, copyright and reproduction	
File reference	OZMOD\REPORTS\R002.DOC
Report number	AEAT/R/ENV/0355
Report status	Issue 1

AEA Technology plc
E6 Culham
Abingdon
Oxfordshire
OX14 3ED
Telephone +44 (0)1235 463118
Facsimile +44 (0)1235 463005

	Name	**Signature**	**Date**
Author	Michael E Jenkin		
Reviewed by	Garry D. Hayman		
Approved by	Garry D. Hayman		

Executive Summary

Ozone is a secondary photochemical pollutant formed from the sunlight-initiated oxidation of volatile organic compounds (VOC, for example hydrocarbons) in the presence of nitrogen oxides (NO_x). Numerical models designed to address the issue of ground level ozone formation therefore require a representation of the emissions of the precursor VOC and NO_X. Existing models tend to assign precursor emission rates at a given location on the basis of annual total emissions, with the assumption that the emission occurs at a constant rate throughout the year. Broadly speaking, however, the emissions can vary on three timescales, namely with season, with day of week and with hour of day. It is probable, therefore, that the implementation of temporal emissions variations may lead to an improvement in the predictive ability of the models.

In the present report, a description is given of a method of assignment of factors which describe the temporal variation of the emissions of VOC and NO_X (and CO and SO_2) on these timescales. A single representative profile has been defined for the diurnal, weekly and annual variations for each pollutant source category, either on the basis of real data or by using one of small set of default profiles. Real data (e.g., fuel consumption, electricity generated, or traffic volumes, which can be related to emissions, and which are themselves temporally resolved) have been used to define temporal emissions variations for road transport, power stations, domestic combustion, decorative paints and natural emissions from forests. On the basis of 1998 NAEI data, these categories collectively account for 40.3%, 70.2%, 79.7% and 71.0% of the emissions of VOC, NO_X, CO and SO_2, respectively. Default profiles have been applied to the remaining source categories, on the basis of our knowledge of, and available information on, the emitting processes, and by consulting trade associations and other interested bodies.

The temporal factors for VOC and NO_X have been incorporated into the Photochemical Trajectory Model (PTM), in conjunction with the 1998 UK emissions defined by the NAEI, and the most recent emissions totals available for other European countries on the EMEP website. The model has been used to investigate the formation of ozone along 96-hour trajectories arriving at 8 southern UK rural sites, for the conditions of a recent ozone episode (31 July 1999), which is reasonably typical of conditions generally associated with photochemical pollution events in the UK. The variation of peak ozone levels at the 8 arrival points with day of week has been determined by performing seven calculations for each trajectory, with the final day corresponding, in turn, to each day of the week. As a direct result of imposing a day of week variation in emissions, the model is able to recreate some of the features of the observed pattern of 90 ppbv exceedences with day of week, which have been reported previously (Jenkin et al., 2000). In particular, Friday is calculated to be the day with the highest peak ozone mixing ratio at 7 of the 8 sites. The calculated peak mixing ratios on each day at each site are used to infer the number of hours exceedence of the 90 ppbv threshold, using a relationship derived from archived monitoring data. The inferred hours exceedence of the 90 ppbv threshold on Friday is calculated to be a factor of two greater than on Monday and Tuesday.

Contents

1 Introduction

During summertime, regional scale photochemical air pollution is a widespread phenomenon across much of north-west Europe. The UK frequently experiences photochemical pollution episodes, which are characterised by high levels of ozone and other photochemical pollutants (e.g., peroxy acetyl nitrate, PAN). The production of elevated levels of ozone is of particular concern, since it is known to have adverse effects on human health, vegetation (e.g., crops) and materials. Established air quality standards for ozone are currently among the most widely exceeded of any pollutant in the UK, and the formulation of control strategies is therefore a major objective of environmental policy.

Ozone is not emitted directly into the troposphere, but is a secondary photochemical pollutant formed from the sunlight-initiated oxidation of volatile organic compounds (VOC, for example hydrocarbons) in the presence of nitrogen oxides (NO_x). The control of ozone formation is thus achieved by the control of emissions of VOC and NO_x. Under conditions characteristic of photochemical pollution episodes, its formation and transport can occur over hundreds of km, with the ozone concentration at a given location influenced by the history of the airmass over a period of up to several days. Consequently, the control of ozone is an international problem requiring solutions agreed at an international level (UNECE, 1992; 1993; 1994).

Numerical models designed to address the issue of ground level ozone formation therefore require a reasonable representation of (i) air mass transport and dispersion, (ii) the emissions of the precursor VOC and NO_X, (iii) the chemical processing of these emissions to generate ozone and other secondary pollutants, and (iv) the removal of ozone and other species by physical processes such as dry deposition. The Department of the Environment Transport and the Regions (DETR) has previously supported the development of such models, which have been successfully applied to investigate the formation and control of ozone on a regional scale over Europe (e.g. Derwent et al., 1996; 1998; Jenkin et al., 1999). Inevitably, some degree of approximation is required for each of the elements (i)-(iv) listed above, if models are to run efficiently. It is important, however, that these approximations are kept under review and periodically updated if this is likely to lead to a significant improvement in the predictive ability of the models.

One area which has recently been reviewed as part of the DETR programmes 'Modelling of Tropospheric Ozone Formation (EPG 1/3/143)' and 'Emission Factors and Cost Curves for Air Pollutants (EPG 1/3/134)' is the temporal dependence of the emissions of the ozone precursors. The previous modelling studies have assigned precursor emission rates at a given location on the basis of annual total emissions, with the assumption that the emission occurs at a constant rate throughout the year. Broadly speaking, however, the emissions can vary on three timescales, namely with season, with day of week and with hour of day. Clearly, a correct description of the seasonal dependence is important, because the photochemical conditions required for ozone formation occur during the summer months. The hour of day dependence is also important, particularly for very reactive VOC which are rapidly oxidised during daylight hours. The variation of emissions with day of week, in conjunction with the multi-day timescale for ozone formation and transport to occur may provide an explanation for the observed prevalence of photochemical ozone episodes on particular days of the week (Jenkin et al., 2000).

In the present report, a detailed description is given of the method of assignment of factors which describe the temporal variation of the emissions of VOC, NO_X, CO and SO_2 on the timescales indicated above. The factors for VOC and NO_X are then incorporated into the Photochemical Trajectory Model (PTM; Derwent et al., 1998), in conjunction with the 1998 UK emissions defined by the NAEI, and the most recent emissions totals available for other

European countries on the EMEP website. The model is used to investigate the formation of ozone along trajectories arriving at 8 southern UK rural sites, for the conditions of a recent ozone episode (31 July 1999). The variation of ozone levels at the arrival points with day of week is determined, and compared with the general pattern observed at rural sites in the UK.

2 Temporal disaggregation of emissions

2.1 METHODOLOGY

The approach adopted in the present study has involved estimating the temporal variations in emissions of VOC, NO_X, CO and SO_2 over the following timescales:

- Diurnal: the portion of daily emissions which occur during each hour of a typical 24 hour period have been estimated.
- Weekly: the portion of weekly emissions which occur on each day of a typical week have been estimated.
- Annual: the portion of annual emissions which occur during each month of a typical year have been estimated.

A single representative profile has therefore been defined for the diurnal, weekly and annual variations for each pollutant source category. Currently, no attempt has been made to identify differences in the diurnal pattern of emissions on different days of the week or at different times of year. Similarly, no attempt has been made to distinguish differences in the weekly pattern of emissions at different times of year. Such differences could well exist: for example, it is conceivable that emissions from decorative paint use and lawn mowers could exhibit a different pattern on a weekend compared with a week-day. In the former case, the emission might be expected to occur throughout the day whereas, in the latter case, emissions might be expected to peak during the early evening, after many people return home from work. Clearly, a fully rigorous temporal profile should therefore define the portion of emissions occurring in each hour of a given year, with the precise profile also changing from one year to the next. However, such a methodology would be impractical, and the resultant information would be difficult to use in modelling applications. The present approach is therefore designed to provide a practical method of defining the temporal variations in emissions.

Two approaches have been used to define the temporal profiles: the use of 'real data' or the use of 'default' profiles. In the first case, we have used data such as fuel consumption, electricity generated, or traffic volumes, which can be related to emissions, and which are themselves temporally resolved. Where possible, real data have been used for source categories making a particularly significant contribution to pollutant emissions (e.g. road transport, power generation). In the second case, we have assumed that emissions follow one of a small set of default profiles. This second approach is used for the greatest number of emission sources since no real data are available.

2.2 DEFAULT PROFILES

The default profiles (listed in Table 1) have been applied, based on our knowledge of, and available information on, the emitting processes. A number of relevant trade associations (given in Appendix 1) and other interested bodies have also been consulted, and we are receiving feedback on the validity of the assumptions made. Where appropriate, the default profiles used for each pollutant source category are given in Table 2.

Table 1: Default profiles used to estimate temporal variations in pollutant emissions

Timescale	Code	Variation
Diurnal	D1	Constant rate throughout the day
Diurnal	D2	Emission over 8 hours, 9 am – 5 pm
Diurnal	D3	Emission over 12 hours, 8 am – 8 pm
Weekly	W1	Emissions occur equally on each day
Weekly	W2	Emissions occur Monday – Saturday only
Weekly	W3	Emissions occur Monday – Friday only
Annual	Y1	Emissions occur equally in each month[1]
Annual	Y2	Emissions occur during April – September only
[1] assigned profiles allow for differing lengths of months		

2.3 REAL DATA

For a number of emissions sectors (also identified in Table 2), it was possible to use real data or established estimation methods to define typical temporal emissions profiles. The source sectors (which are often made up of several component sub-sectors, e.g. fuel and vehicle type in the case of road transport) are also listed in Table 3. This table shows that real data were used to assign profiles to a substantial proportion of the total emissions of each pollutant.

The emissions from road transport were calculated using the NAEI road transport emissions model. The methodology involved combining emission factors with hourly and daily traffic flow data, taken from DETR's Road Traffic Statistics Great Britain 1992. This allowed the variation in hot exhaust emissions by hour of day and day of week to be estimated. Average temperature and diurnal temperature fluctuation data, from the Meteorological Office were used to estimate the temporal behaviour of cold-start and evaporative emissions by hour of day. Trends in average monthly traffic flows and temperature, together with seasonal changes in fuel vapour pressure, were used to estimate the variation in monthly emissions. The same data and methodology are used to generate the quarterly toxic tailpipe emission indices published by the Automobile Association.

Figures 1-3 show the relative temporal profiles for exhaust and evaporative VOC emissions from the various road transport fuel and vehicle categories. These data show some interesting variations, reflecting competing trends in a number of factors. The bulk of exhaust emissions of all pollutants show a slight downward trend during the course of a year, due to the gradual penetration of newer, lower emitting vehicles in the fleet, and the phasing out of older vehicles. However, this downward trend is partially offset in the latter part of the year, by elevated levels in winter months due to cold-start emissions, generally leading to a late summer/autumn minimum in exhaust emissions. In the case of VOC, significantly higher levels of evaporative losses occur during the summer months, which more than compensate for the lower exhaust emissions. Consequently, total VOC emissions from road transport tend to maximise in the summer (see Figure 1), whereas NO_X, CO and SO_2 minimise in the late summer/autumn.

Table 2: Summary of profiles assigned to pollutants source categories

Source	Fuel	Diurnal	Weekly	Annual
Agrochemicals use[1]		D3	W1	Y1
Aircraft	All fuels	D1	W1	Y1
Alcoholic drink[1]		D1	W1	Y1
Cement & lime	All fuels	D1	W1	Y1
Chemicals manufacture[1]		D1	W1	Y1
Coating (coil)[1]		D1	W2	Y1
Coating (film)[1]		D1	W2	Y1
Coating (heavy duty)[1]		D2	W3	Y1
Coating (leather)[1]		D2	W3	Y1
Coating (metal packaging)[1]		D1	W2	Y1
Coating (new vehicles)[1]		D1	W2	Y1
Coating (textile)[1]		D1	W2	Y1
Coating (vehicle refinishing)[1]		D2	W3	Y1
Coating (wood)[1]		D2	W3	Y1
Coating manufacture[1]		D2	W3	Y1
Coatings (marine)[1]		D2	W3	Y1
Coatings (metal & plastic)[1]		D2	W3	Y1
Coke & SSF production	All fuels	D1	W1	Y1
Combustion (agriculture)	All fuels	D1	W1	Y1
Combustion (domestic)	Liquid/gaseous fuels	D1	W1	**Real Data**
Combustion (domestic)	Solid fuels	D3	W1	**Real Data**
Combustion (industry)	All fuels	D1	W1	Y1
Combustion (power generation)	All fuels	**Real Data**	**Real Data**	**Real Data**
Combustion (commercial)	All fuels	D2	W3	Y1
Decorative paints[1]		D3	W1	**Real Data**
Domestic solvent use (aerosols etc.)[1]		D3	W1	Y1
Dry cleaning[1]		D2	W3	Y1
Field burning		D3	W1	Y2
Food industry (bread baking)[1]		D1	W1	Y1
Food industry (other)[1]		D2	W3	Y1
Forests[1]		**Real Data**	W1	**Real Data**
Garden equipment	All fuels	D3	W1	Y2
Gas leakage[1]		D1	W1	Y1
Incineration	All fuels	D1	W1	Y1
Industrial adhesives[1]		D2	W3	Y1
Iron and steel (all sources)	All fuels	D1	W1	Y1
Landfill[1]		D1	W1	Y1
Off-road vehicles (agriculture)	All fuels	D3	W1	Y1

Source	Fuel	Diurnal	Weekly	Annual
Off-road vehicles (airport)	All fuels	D1	W1	Y1
Off-road vehicles (industry)	All fuels	D2	W3	Y1
Oil and gas production		D1	W1	Y1
Other solvent use[1]		D1	W1	Y1
Petrol distribution (petrol stations)[1]		D2	W3	Y1
Petrol distribution (refineries & terminals)[1]		D1	W1	Y1
Petrol distribution (vehicle refuelling)[1]		D3	W1	Y1
Printing (flexography, gravure, heatset)[1]		D1	W2	Y1
Printing (newspaper inks)[1]		D1	W1	Y1
Printing (screen printing & other inks)[1]		D2	W3	Y1
Railways (locomotives)	All fuels	D1	W1	Y1
Railways (stationary sources)	All fuels	D1	W1	Y1
Refineries (all sources)	All fuels	D1	W1	Y1
Road construction		D1	W1	Y2
Road transport	All fuels	**Real Data**	**Real Data**	**Real Data**
Rubber goods manufacture[1]		D2	W3	Y1
Seed oil extraction[1]		D1	W1	Y1
Shipping	All fuels	D1	W1	Y1
Surface cleaning[1]		D2	W3	Y1
Wood impregnation[1]		D1	W1	Y1

[1] These source categories apply to VOC emission only: the remaining source categories apply to emissions of VOC, NO_X, CO and SO_2

Table 3: Percentage contributions to total emissions made by sectors for which real temporal emissions data were used

	VOC	NO_X	CO	SO_2
Decorative Paints	2.1 %	-	-	-
Domestic Combustion	1.9 %	4.0 %	4.9 %	3.2 %
Forests	9.1 %	-	-	-
Power Stations	0.3 %	20.7 %	1.5 %	66.4 %
Road Transport	26.9 %	45.5 %	73.3 %	1.4 %
Total	**40.3 %**	**70.2 %**	**79.7 %**	**71.0 %**

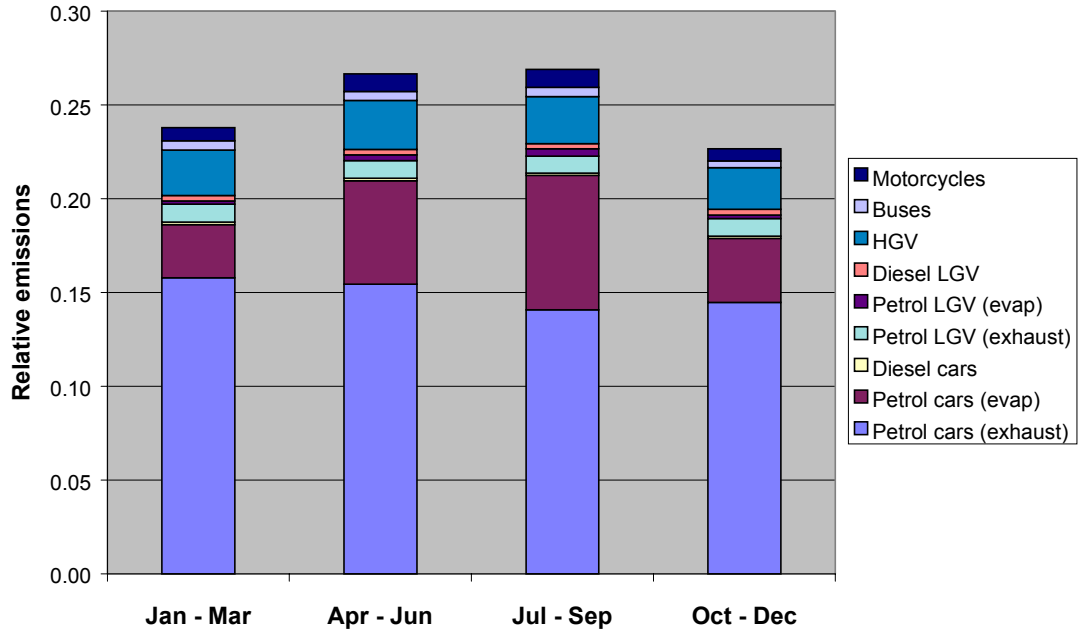

Figure 1: Relative VOC emissions of road transport categories with season

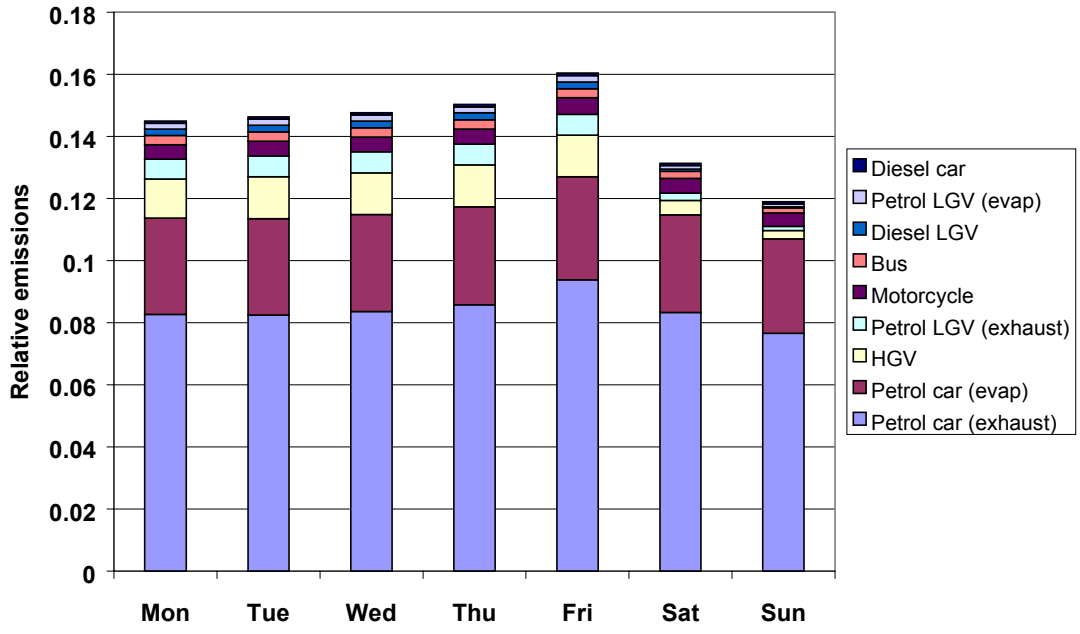

Figure 2: Relative VOC emissions of road transport categories with day of week

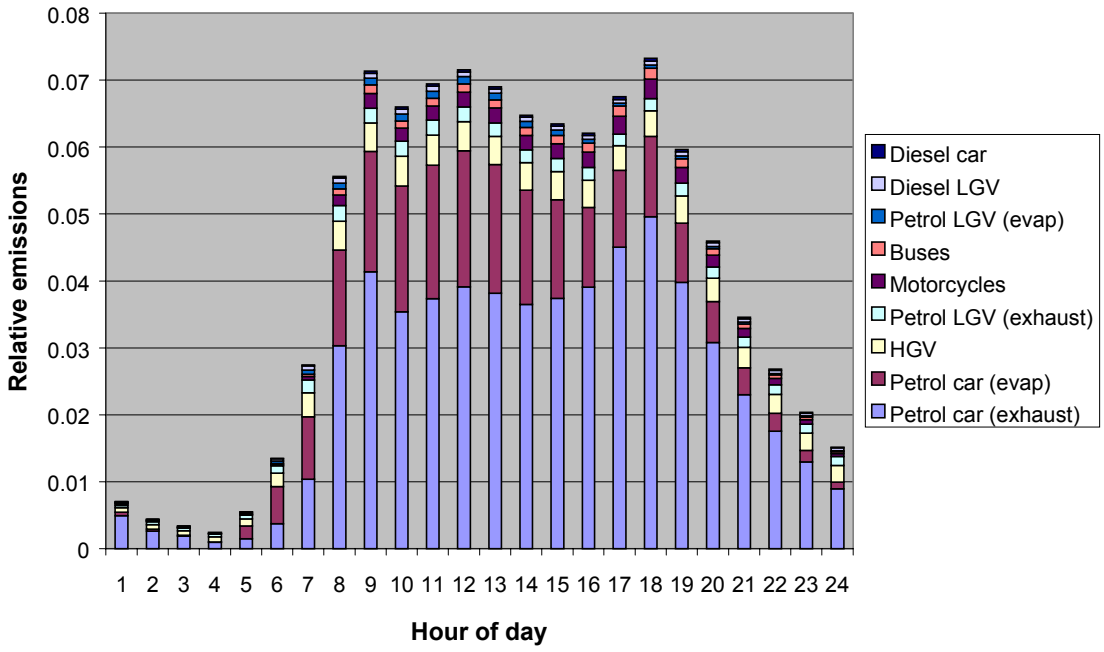

Figure 3: Relative VOC emissions of road transport categories with hour of day

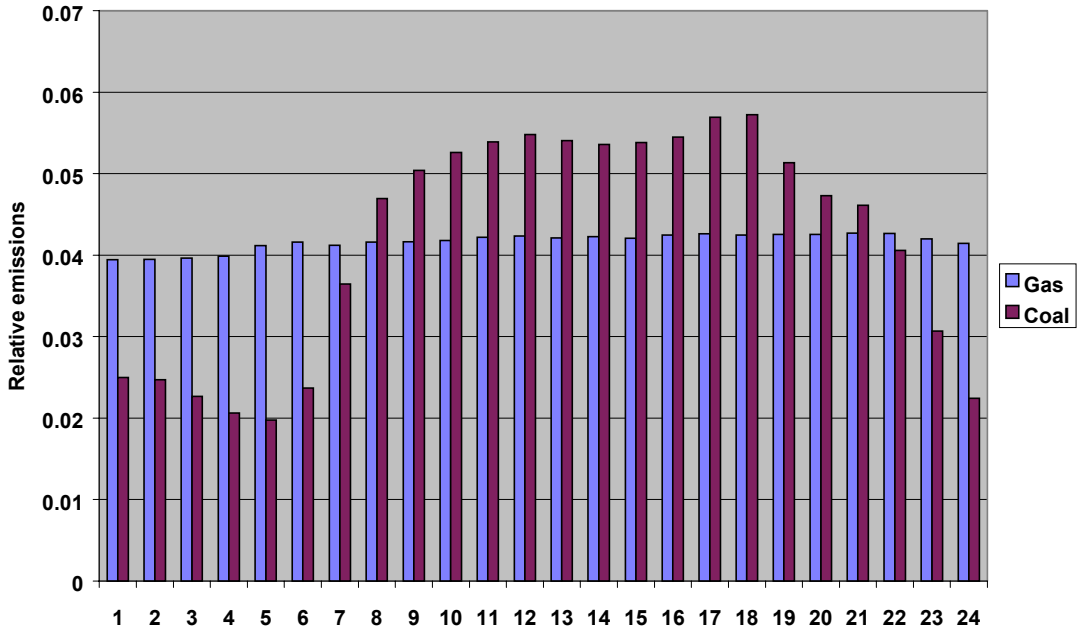

Figure 4: Relative diurnal emissions from power generation by coal and gas combustion.

Temporal factors were assigned to power generation by coal combustion (and related sectors) and natural gas combustion (and related sectors) on the basis of data from a number of sources. For both coal and natural gas combustion, the hour of day and day of week profiles were based on data provided by the National Grid, some of which is also presented in their 7 year statement (National Grid, 1999). The resultant diurnal profiles are shown in Figure 4. In the case of natural gas combustion, there is no significant variation on either of these timescales, and the defaults D1 and W1 can reasonably be applied. The month of year factors were determined for coal and natural gas combustion on the basis of typical demand data for summer and winter supplied by the National Grid, and quarterly data on the usage of fuel in electricity generation, as presented in the DTI Energy Trends publication.

Data presented in the DTI Energy Trends publication on the monthly use of coal and gas in domestic combustion over the period 1995-1997 were also used to define the month of year profiles. As indicated in Table 1, the diurnal and day of week variations for domestic combustion were assigned defaults.

The annual and diurnal emissions of natural hydrocarbons from forests were also defined on the basis of available data, with the day of week assigned default W1 (Table 1). The annual and diurnal variations account for the variations in light (photosynthetically active radiation, PAR) and temperature, by making use of the published methodology of Guenther et al (1994) as also discussed for Europe by Simpson et al (1995). For this procedure, it was assumed that the emissions were entirely in the form of isoprene, which is consistent with the current representation in ozone models (Derwent et al., 1998). The month of year temperature variation was based on data given in DUKES (1999). The hour of day variation was based on a standard diurnal temperature variation currently adopted in boundary layer models (Derwent et al., 1998). The variation of PAR was inferred from the time of year and hour of day variation of actinic flux determined from photolysis models (Hough 1988).

Month of year emissions for decorative paint sectors were assigned on the basis of the monthly profile of paint sales compiled by Passant and Lymberidi (1998). As indicated in Table 1, the corresponding diurnal and day of week were assigned defaults.

2.4 COMPOSITE TEMPORAL EMISSIONS PROFILES

Provided total annual emissions estimates are available for a given location, the temporal codes defined in the present work allow the emissions rates of VOC, NO_X, CO and SO_2 to be estimated for each hour of the year for either all sectors, or for specific sectors or sectoral combinations. As an illustration, the profiles have been used to generate composite data for each pollutant (see Figures 5-7). These figures show how the total emissions of each pollutant vary on the three timescales, but also indicate the contributions to these totals made by a number of broad emissions categories: solvent use (VOC only), road transport, industry/processes, natural (VOC only), fossil fuel distribution, domestic combustion, power generation and other sources.

Although the composite profiles generally show a similar pattern from one pollutant to another, there are some interesting differences. Figure 5 demonstrates that VOC emissions alone maximise in the summer months. As indicated above, this is partially as a result of increased evaporative road transport emissions, but also due to the majority of the natural VOC emissions occurring in the summer months. Clearly, therefore, the application of the seasonal emissions variations will have a notable influence on the relative emissions of VOC and NO_X during the photochemical season.

As shown in Figure 6, the emissions of all four pollutants are estimated to be substantially lower at weekends, the emissions being in the region of 70-80% of the weekday values. Figure 7 demonstrates that the emissions of all the pollutants are also estimated to have a significant

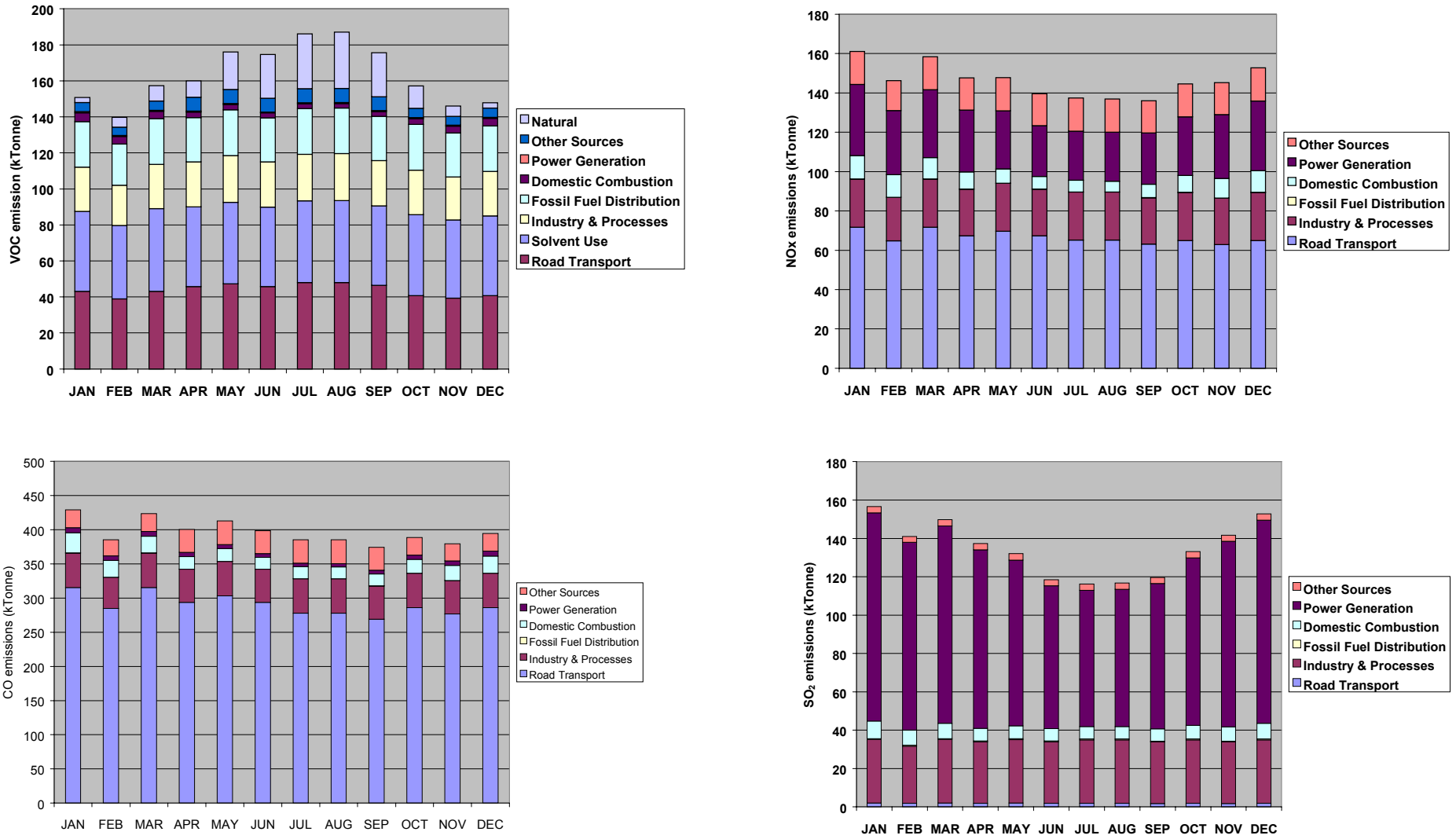

Figure 5: Variation of emissions of VOC, NO_X, CO and SO_2 with month of year, based on 1998 totals defined by the NAEI. Note that the presented variation reflects the differing lengths of the months

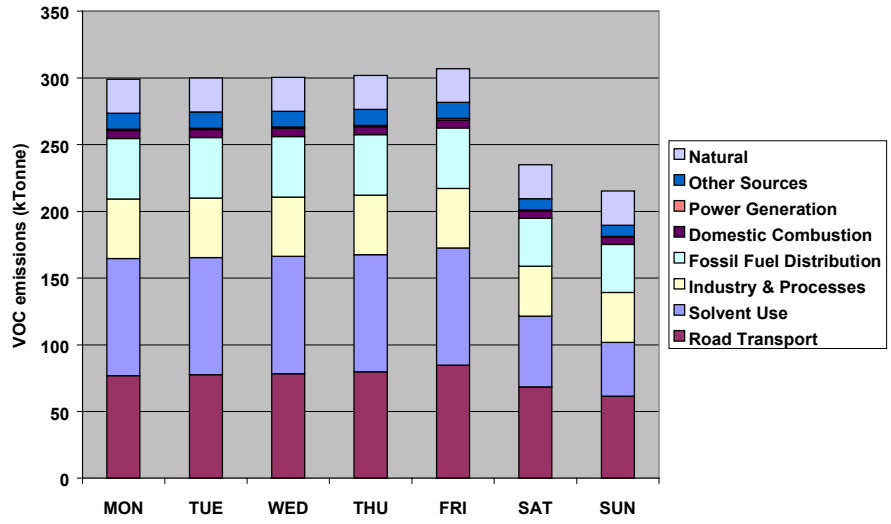

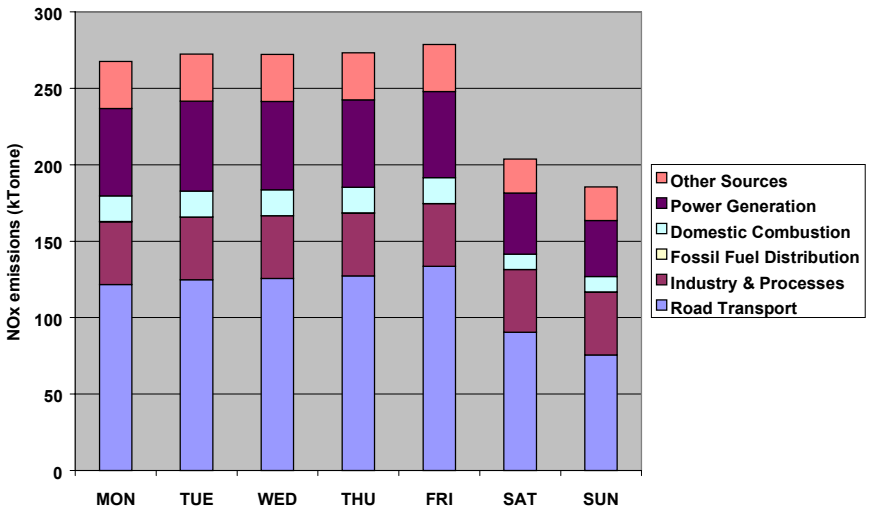

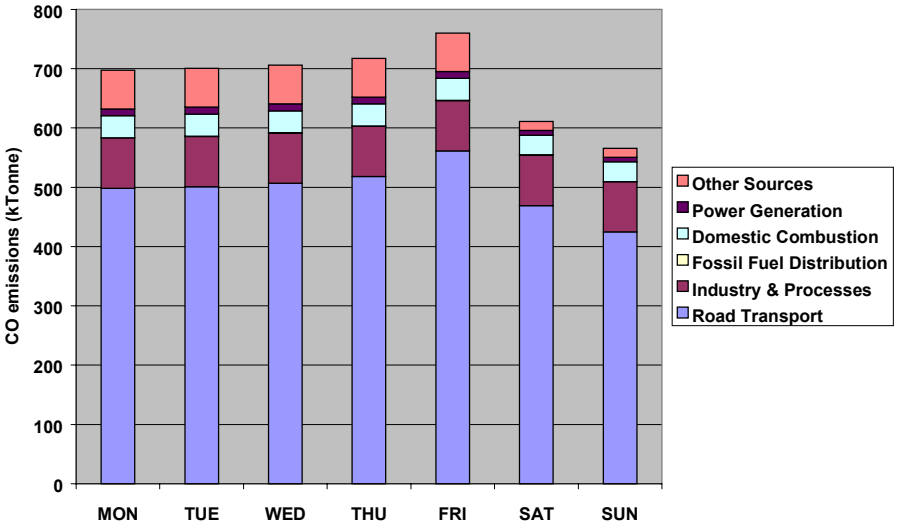

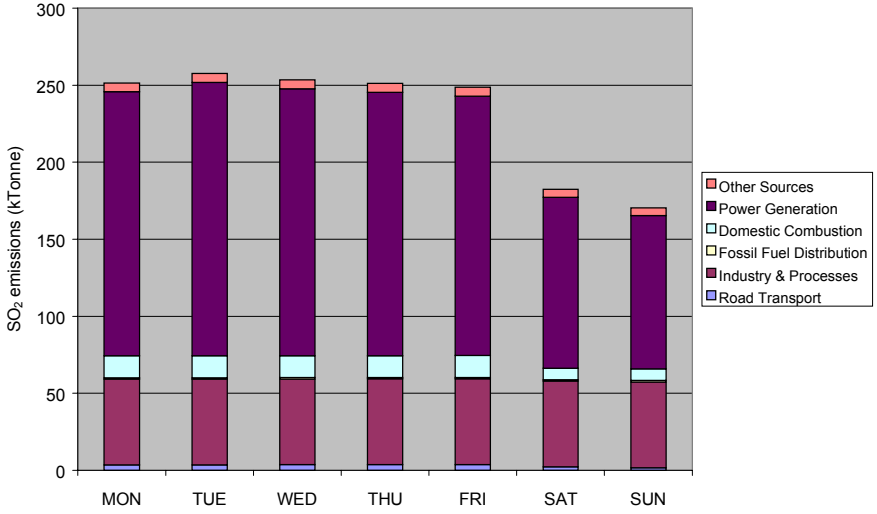

Figure 6: Variation of emissions of VOC, NO_X, CO and SO_2 with day of week, based on 1998 totals defined by the NAEI.

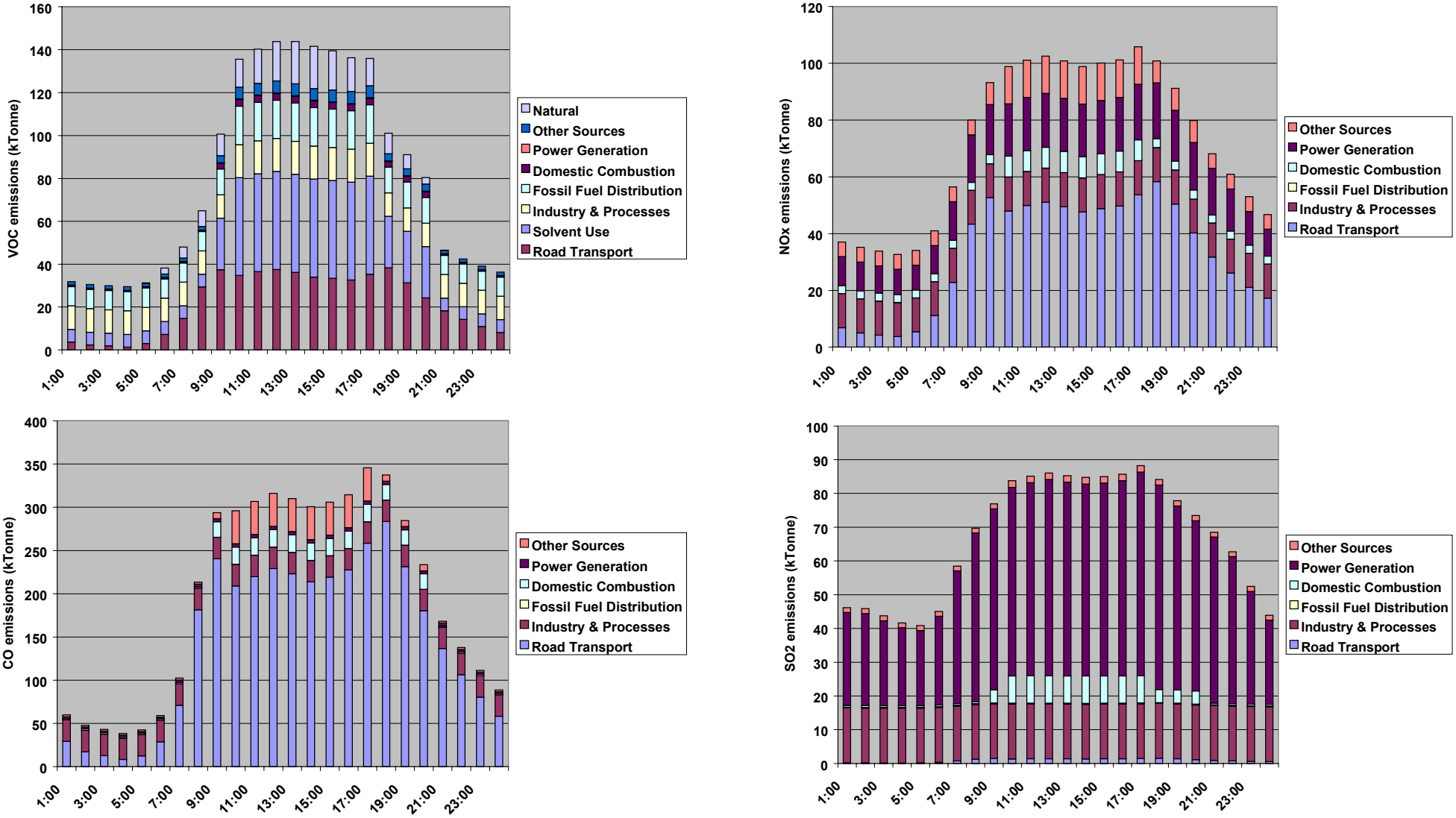

Figure 7: Variation of emissions of VOC, NO_X, CO and SO_2 with hour of day, based on 1998 totals defined by the NAEI.

diurnal profiles. For VOC, NO_X and CO, a strong contribution to this variation results from road transport emissions. In the case of SO_2 emissions, the major contributor is the combustion of coal in power generation.

3 Temporal dependence of ozone exceedences

3.1 INTRODUCTION

Jenkin et al (2000) have recently carried out an analysis to investigate the number of hours the 90 ppbv ozone information threshold was reached or exceeded on each day of the week at 14 rural sites in the UK over the period 1989-1999. The results demonstrated that there is a distinct temporal pattern, repeated at many of the sites, which indicate that ozone exceedences are more prevalent towards the end of the week. Data for five of the long-running southern UK rural sites (i.e. those collecting data throughout the period 1989-1999) considered in that study are reproduced in Figure 8, together with the total for all the rural sites considered.

As shown in the figure, the number of hours of exceedence clearly maximises on Fridays, with Saturdays and Thursdays also having a significantly greater number of hours than other days. A similar pattern is also obtained at many of the individual sites. For example, 4 of the 5 sites for which data are given in Figure 8 have the greatest number of hours exceedence on Fridays, with the remaining site having slightly more on Saturdays. However, there are some interesting differences between the sites. Those further to the west (Yarner Wood and Aston Hill) have a well defined single maximum at the end of the week (Thursday – Saturday), whereas the central southern UK site (Harwell), and those to the east (Sibton and Lullington Heath) appear to have an additional maximum earlier in the week.

The prevalence of ozone episodes towards the end of the week is almost certainly a consequence of a day of week dependence of ozone precursor emissions. Other factors which contribute to the occurrence of ozone episodes are either invariant with day of week (i.e. in the case of chemical parameters) or are equally likely to occur on each day of the week (i.e. in the case of appropriate meteorological conditions). The temporal profiles presented in Figure 6 clearly demonstrate that precursor VOC and NO_X emissions are generally greater on weekdays than on weekend days. Consequently, for identical meteorological conditions, it is likely that the rate of ozone production is greater on weekdays than it is on weekend days. If the ozone concentration at a given point under summertime anticyclonic conditions is assumed to be influenced by the airmass history over a period of about five days (i.e. typical of transport times across Europe), then a day of week dependence in peak ozone concentration would indeed be expected, with the maximum occurring on Friday. This is essentially because the integrated precursor emissions over a five day period are greater for the period Monday-Friday than for any other five day period. To test this hypothesis, the Photochemical Trajectory Model (PTM) has been used to investigate the formation of ozone along trajectories arriving at 8 southern UK rural sites, for the conditions of a recent ozone episode (31 July 1999).

3.2 A CASE STUDY OF 8 RURAL SITES: 31 JULY 1999

The most severe UK photochemical ozone episode in 1999 occurred at the end of July and beginning of August, with highest aggregate concentrations measured at rural sites on Saturday 31 July. This date was therefore selected for a case study, using the 8 southern UK rural sites listed in Table 4. The 8 sites include the 5 long-running sites for which data are presented in

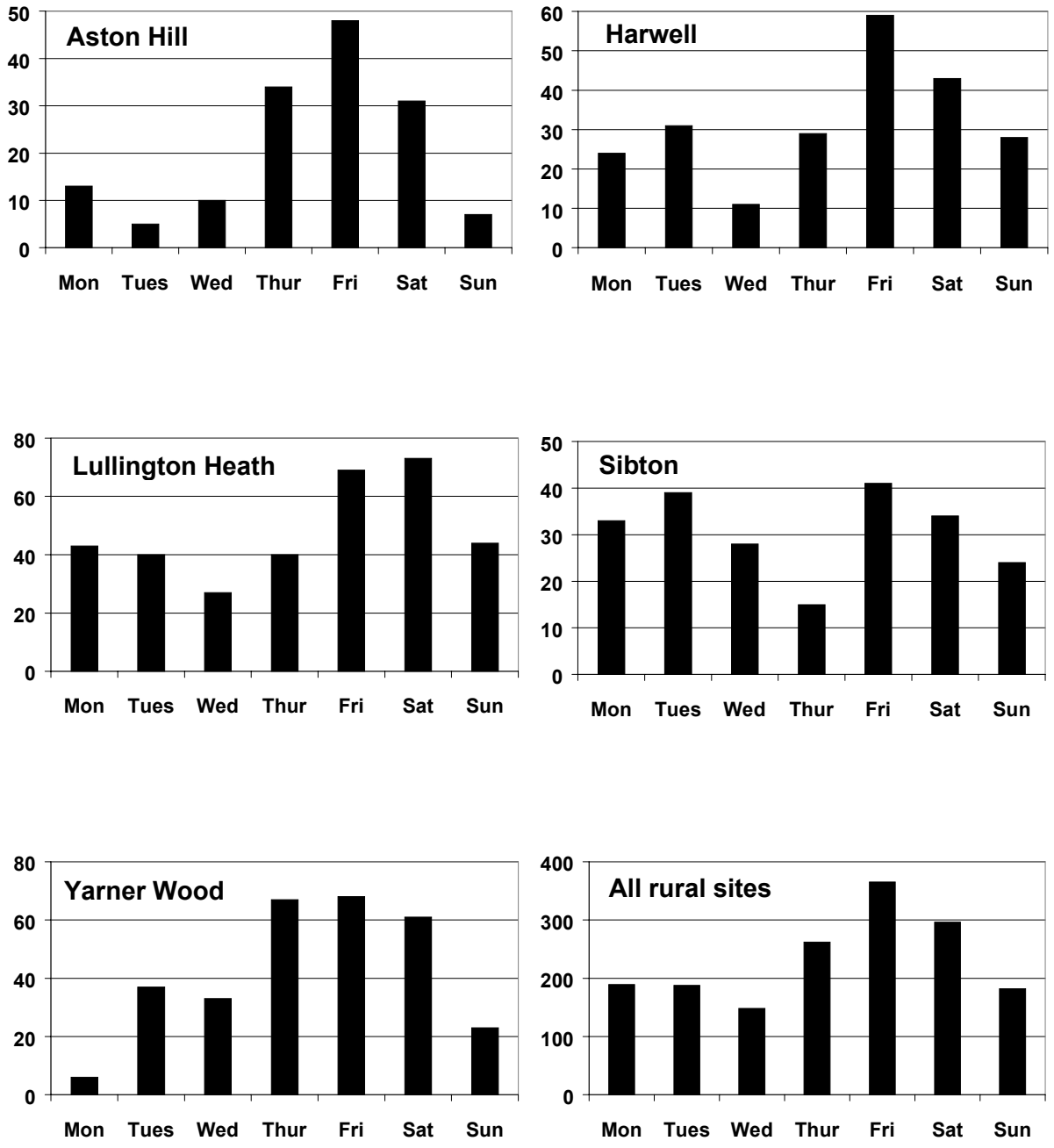

Figure 8: Number of hours with ozone ≥ 90 ppbv on each day of the week at selected long-term rural sites in the UK over the period 1989-1999, and the total number of hours by day of week at all 4 rural sites considered by Jenkin et al. (2000). The sites for which data are shown are in Devon (Yarner Wood), Oxfordshire (Harwell), Powys (Aston Hill), Suffolk (Sibton) and Sussex (Lullington Heath).

Table 4: Observed peak ozone mixing ratios at 8 southern UK sites on Saturday 31 July 1999, and those simulated using the Photochemical Trajectory Model

Site	Observed peak ozone (ppbv)[1]	Simulated peak ozone (ppbv)[2]
Aston Hill (Powys)	98	93.9
Harwell (Oxfordshire)	100	92.0
Lullington Heath (Sussex)	111	102.0
Rochester (Kent)	92	101.5
Sibton (Suffolk)	Not measured	102.2
Somerton (Somerset)	89	88.5
Wicken Fen (Cambridgeshire)	92	81.3
Yarner Wood (Devon)	77	68.7
[1] based on hourly mean; [2] see text		

Figure 8. As indicated in Table 4, elevated ozone levels were recorded throughout the southern UK, with peak levels exceeding the 90 ppbv threshold at 5 sites.

The meteorological conditions on 31 July 1999 were typical of those generally associated with elevated levels of ozone in the UK. A recent analysis of airmass origins associated with ozone episodes (Jenkin et al., 2000) clearly demonstrates that the highest levels of ozone at the UK sites tend to occur when the back trajectories have 'looped' over mainland Europe and arrive in the UK from a broadly easterly or south-easterly direction. Under such conditions, the airmass receives a plentiful supply of ozone precursor emissions (i.e. VOC and NO_X) from populated regions during a period of several days prior to arrival at the UK sites. Given that such trajectories are also typical of those established during stable anticyclonic conditions, the corresponding high solar intensity promotes the photochemical processing of the emissions which leads to ozone generation.

Figure 9 shows the 96-hour trajectories arriving at Aston Hill and Harwell at 1600 hr on 31 July 1999. The trajectories arriving at all 8 sites are provided in Appendix 2. Clearly, these are typical of the description given above. It should also be noted that, for the prevalent conditions, the Harwell site was positioned directly downwind of London, and therefore was influenced by a large injection of pollution comparatively late in the trajectory.

3.3 SIMULATION OF OZONE FORMATION ON 31 JULY 1999

3.3.1 The Photochemical Trajectory Model

The Photochemical Trajectory Model (PTM) used in the present study was based on that which has been widely applied to the simulation of photochemical ozone formation in north-west Europe (e.g., Derwent et al., 1996; 1998). The PTM simulates the chemical development in a boundary layer air parcel travelling along pre-selected trajectories over Europe. The air parcel thus picks up emissions of NO_X, CO, SO_2, methane, non-methane VOCs and biogenic isoprene (based on available emissions inventories), which are processed using an appropriate description of the chemical and photochemical transformations leading to ozone formation.

Aston Hill

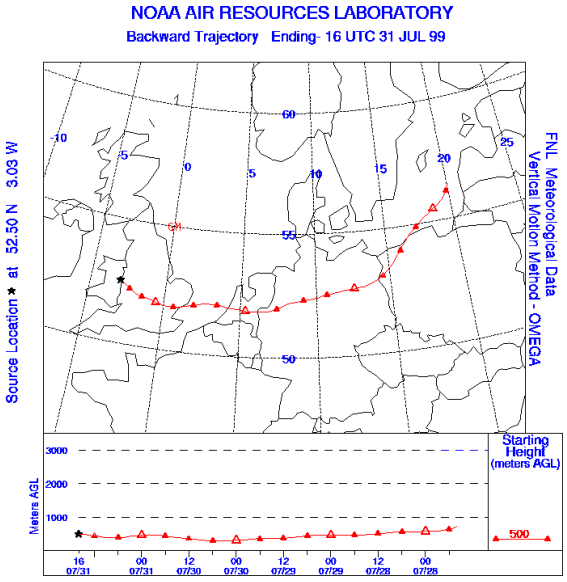

Harwell

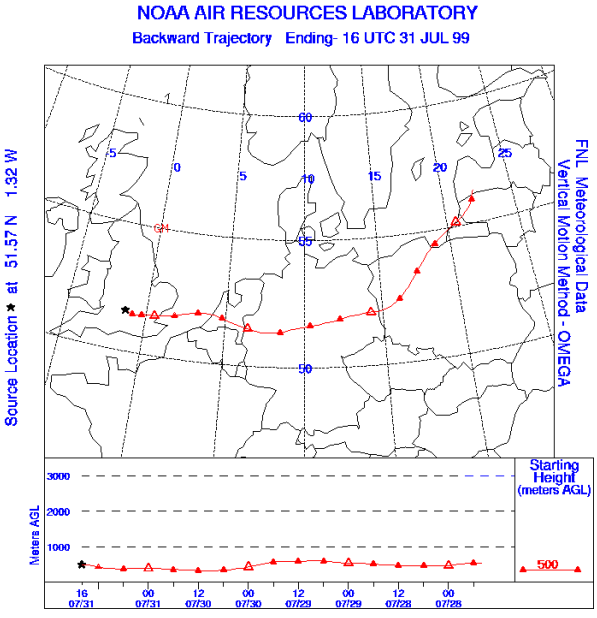

Figure 9: 96-hour trajectories arriving at Aston Hill and Harwell at 1600 hr on 31 July 1999

The PTM sets up a differential equation of the following form for the concentration (C_i) of each of the model species, i, in the mechanism,

$$\frac{dC_i}{dt} = P_i - L_i.C_i + \frac{E_i}{h} - (C_i - B_i)\frac{1}{h}\frac{dh}{dt} - \frac{V_i C_i}{h} \qquad (i)$$

where the respective terms represent the production and loss by chemistry, the emissions of pollutants into the air parcel, the exchange of pollutants from the free troposphere above the air parcel and dry deposition of the pollutant to the underlying surface. The equations are integrated for the duration of the trajectory. Diurnal variations in atmospheric boundary layer depths, windspeeds, temperatures and humidities are represented as climatological means over a number of photochemical episodes. For a small number of species, initial concentrations are set at realistic tropospheric baseline levels for north-west Europe.

For the present investigation, a number of updates were made to the model. The UK emissions inventories for VOC, NO_X, CO and SO_2 were updated to the 1998 figures supplied by the NAEI. For other European countries, the existing inventories (based on EC CORINAIR and EMEP) were scaled so that the country totals were consistent with the latest figures available on the EMEP website (generally corresponding to 1997). The total emissions of VOC and NO_X were varied temporally in accordance with the profiles presented in Figure 5-7.

The chemical processing was achieved using the Common Representative Intermediates (CRI) Mechanism, which has been described recently by Jenkin et al. (2000). The CRI mechanism treats the degradation of 120 emitted VOC using about 570 reactions of 250 species. It provides an economical alternative to the near-explicit representation in the Master Chemical Mechanism (ca. 10,500 reactions of ca. 3,500 species for 123 VOC), thereby allowing a large number of trajectory calculations to be carried out comparatively efficiently. As the name suggests, the CRI mechanism contains a series of generic intermediate radicals and products, which mediate the breakdown of larger VOC into smaller fragments (e.g., formaldehyde), the chemistry of which is treated explicitly. Initial testing of the mechanism in the PTM on a standard five-day trajectory (Jenkin et al., 2000) has demonstrated that the CRI mechanism generates levels of ozone which are in excellent agreement with those calculated on the same trajectory using MCM v2.0.

The model was used to simulate the chemical development over a 96 hour period along the 8 trajectories arriving at the southern UK sites at 1600 hr (Figure 9 and Appendix 2). The trajectories were obtained from the NOAA interactive on-line trajectory service (http://www.arl.noaa.gov/ready/hysplit4.html). The model was therefore initialised at 1600 hr on day 1 of the trajectory, arriving at the end point at 1600 hr on day 5.

3.3.2 Results and Discussion

To allow comparison of simulated and observed ozone levels, the model was initially run such that the trajectories were initialised with day 1 as Tuesday and with arrival at the end point on Saturday. The corresponding time evolution of ozone along selected trajectories is shown in Figure 10. The simulated mixing ratios at the end points for all 8 trajectories are compared with those observed at all sites in Table 4 and Figure 11. In general terms, the agreement is reasonably good, with the difference between observed and calculated levels (obs-calc) ranging from –9.5 ppbv at Rochester to +10.7 ppbv at Wicken Fen. For the 7 sites for which comparison is possible, the model correctly calculates Lullington Heath to have the highest ozone mixing ratio, and Yarner Wood to have the lowest.

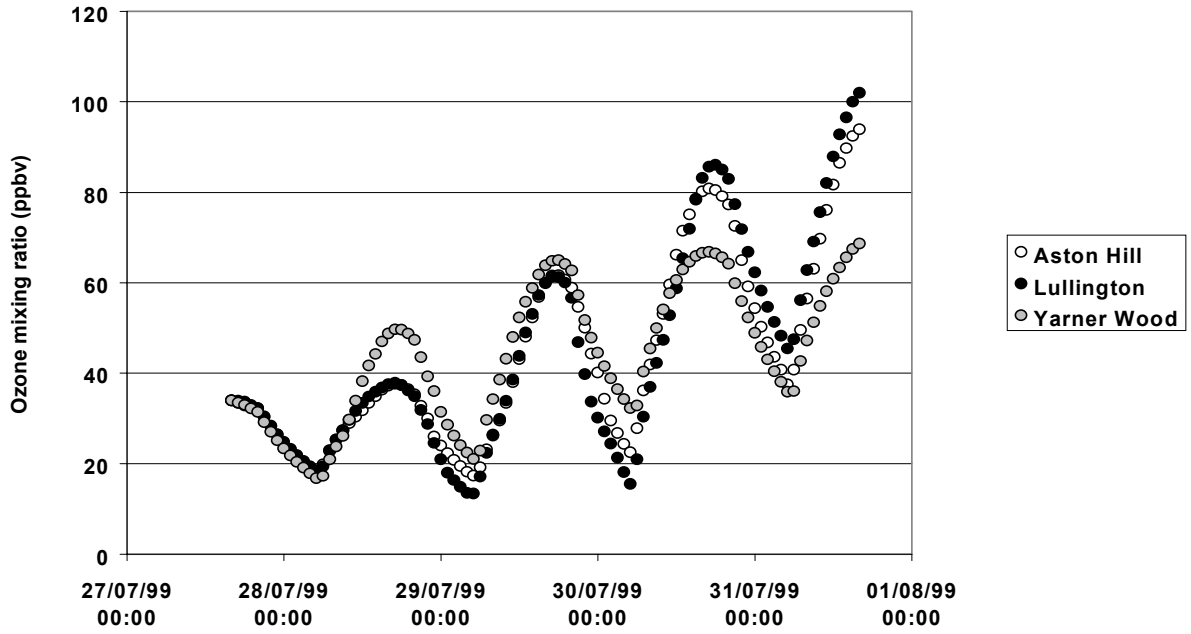

Figure 10: Simulated time evolution of ozone over a 96-hour period prior to arrival at Aston Hill, Lullington Heath and Yarner Wood at 1600 hr on Saturday 31 July 1999. In each case, the ozone mixing ratio was initialised at a regional background level of 34 ppbv.

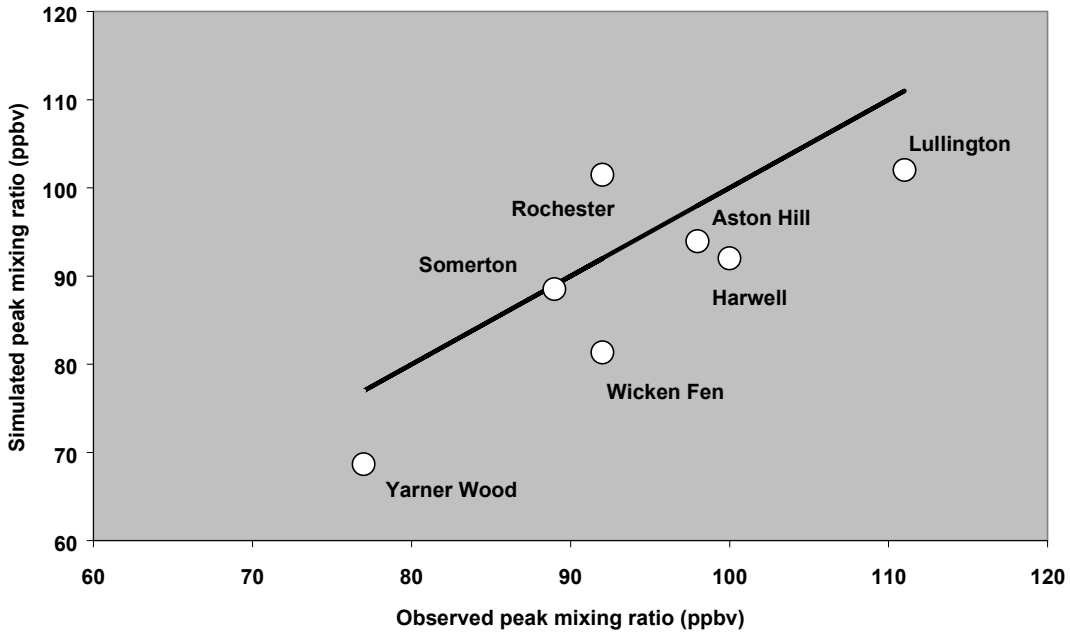

Figure 11: Comparison of simulated and observed peak ozone mixing ratios at southern UK sites for Saturday 31 July 1999. The line is a 1:1 correspondence.

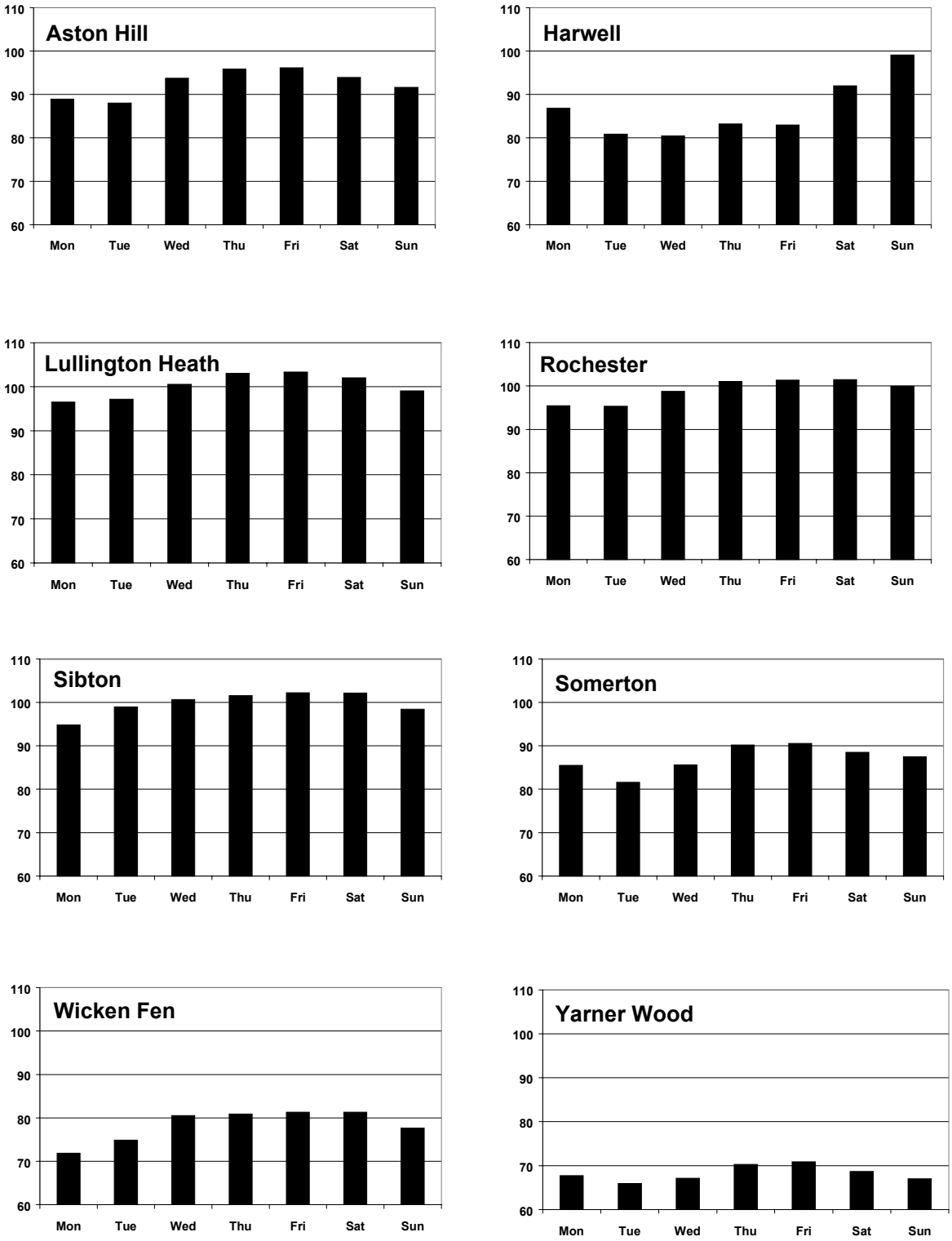

Figure 12: Variation of simulated peak ozone mixing ratios (in ppbv) at 8 southern UK sites with day of week. Plots show mixing ratios in excess of 60 ppbv.

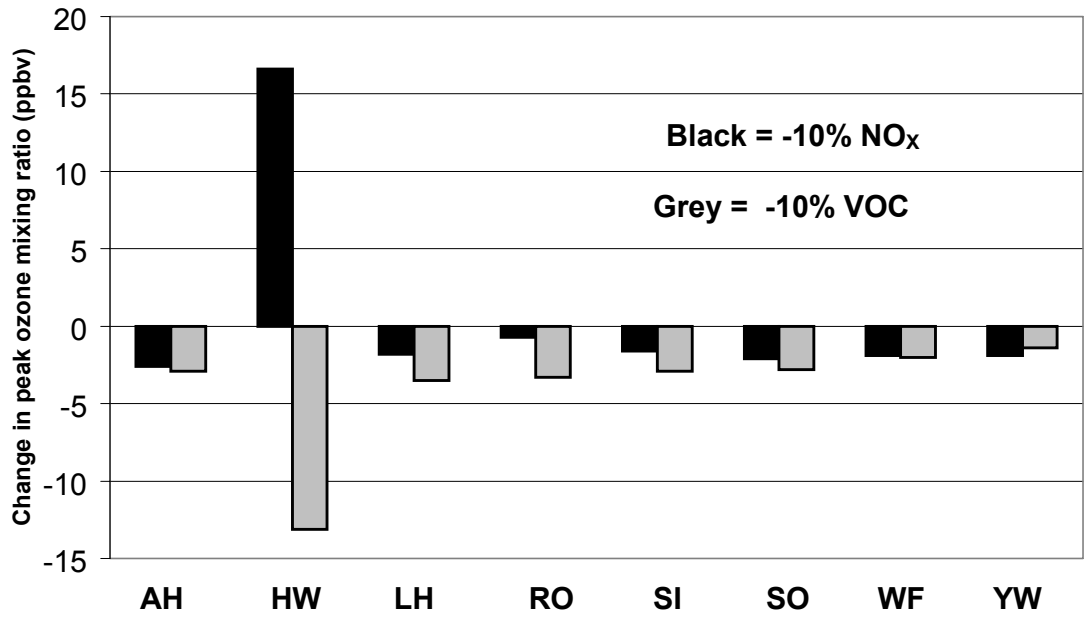

Figure 13: Change in simulated peak ozone mixing ratios at 8 southern UK sites with 10% reductions in VOC or NO_X emissions throughout Europe, for the conditions of 31 July 1999.

The influence of artificially varying the arrival day was then investigated. Seven calculations were therefore performed for each trajectory to calculate the peak ozone mixing ratio at each site, with the final day corresponding, in turn, to each day of the week. The results are shown in Figure 12. With the exception of Harwell, all sites show a similar pattern, with the highest mixing ratio generally calculated for arrival on a Friday. For Rochester and Sibton, however, the mixing ratios calculated for Friday and Saturday are essentially identical, with that calculated for Thursday only very marginally lower. The minimum calculated peak ozone at these sites (usually on a Monday or Tuesday) is typically about 7 or 8 ppbv lower. The calculations for Harwell show a distinctly different pattern to those observed at the other sites, with significantly higher peak ozone levels calculated on Saturday and Sunday. As mentioned above (and shown in Figure 8), the trajectory to Harwell on 31 July 1999 passes directly over central London a few hours before arrival, and therefore receives a significant injection of pollution comparatively late in the trajectory. Under these circumstances, the air mass is strongly VOC limited, with ozone production being very sensitive to the VOC/NO_X ratio and also inhibited by high absolute levels of NO_X. Consequently, the ozone formation in the latter stages of the trajectory is calculated to be greater on the weekend days when the absolute levels of NO_X injected as the air mass passes over London are lower.

The ozone formation characteristics along the trajectories to all the sites were investigated by performing additional calculations in which the emissions of anthropogenic VOC and NO_X were reduced, in turn, by 10% throughout the whole model domain (arrival day Saturday). The results presented in Figure 13 show clearly that the trajectory to Harwell is strongly VOC-limited, with a significant decrease in the calculated ozone concentration when VOC emissions are reduced, and a significant increase when NO_X emissions are reduced. The other sites are less sensitive to the controls, but all show modest reductions in ozone when either precursor is

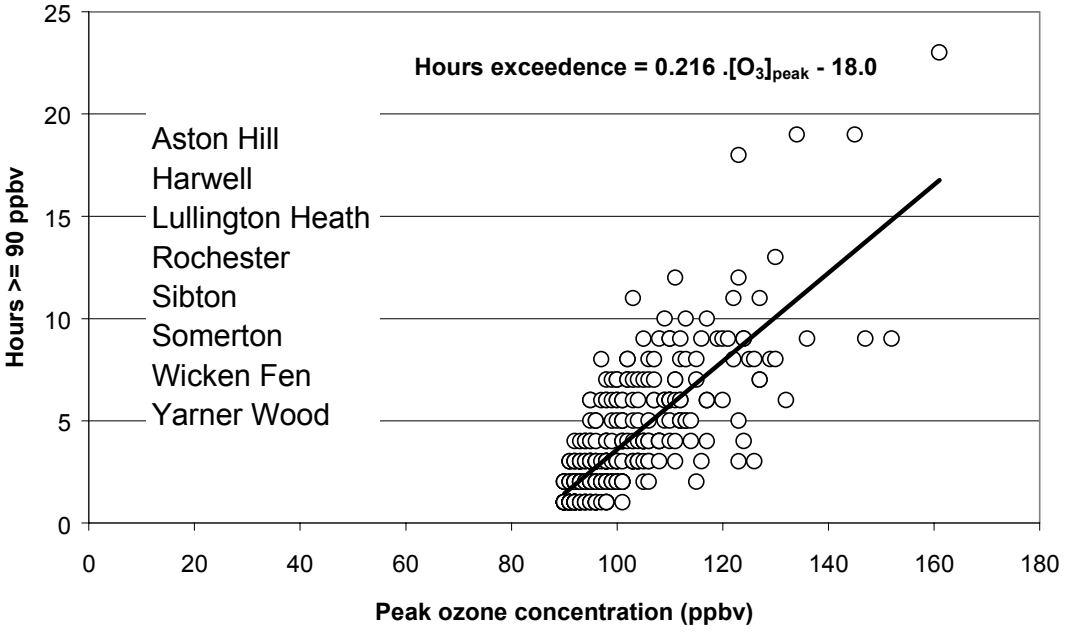

Figure 14: The observed relationship between the peak ozone mixing ratio (≥ 90 ppbv) in a given episode and the number of consecutive hours ≥ 90 ppbv, on the basis of data from the 8 rural sites over the period 1989-1999.

reduced, with VOC reductions generally having a slightly greater effect. This suggests that the southern UK generally benefits from reductions in either precursor.

In general terms, the results presented in Figure 12 are consistent with the observed prevalence of ozone episodes on Fridays, as the highest peak ozone level is calculated for Fridays at most sites. However, the observational statistics are in terms of the 'number of hours the 90 ppbv threshold is reached or exceeded', whereas the PTM output defines an instantaneous peak mixing ratio at the end point of a trajectory. Data from the air quality archive was therefore analysed to see if there is a relationship between observed peak ozone mixing ratio, and the number of consecutive hours a given threshold is exceeded. Data for the 8 rural sites considered in the present study over the period 1989-1999 are presented in Figure 14. These show there is a distinct relationship between the peak ozone mixing ratio (≥ 90 ppbv) in a given episode and the number of consecutive hours ≥ 90 ppbv. Although the plot shows a significant amount of scatter, it implies that the two quantities may be related by the following expression, when averaged over a large number of events:

$$\text{Hours} \geq 90 \text{ ppbv} = 0.216.[O_3]_{peak}(\text{ppbv}) - 18.0 \qquad \text{(ii)}$$

This expression was used, therefore, to infer the number of hours ≥ 90 ppbv at each of the 8 sites, from the calculated ozone peak values. The results for the 6 sites where the 90 ppbv threshold was calculated to be achieved on at least one day of the week are shown in Figure 15, along with the combined total for these sites. The total for all sites recreates some of the features of observed pattern of exceedences with day of week shown for all rural sites in Figure 8. In particular, Friday is identified as the day with most hours exceedence, the inferred number of hours being a factor of two greater than on Monday and Tuesday. Certain other features are not recreated, however, in particular the comparatively small number of hours exceedence observed on Wednesdays and Sundays (Figure 8). Although the 31 July 1999 episode is reasonably typical

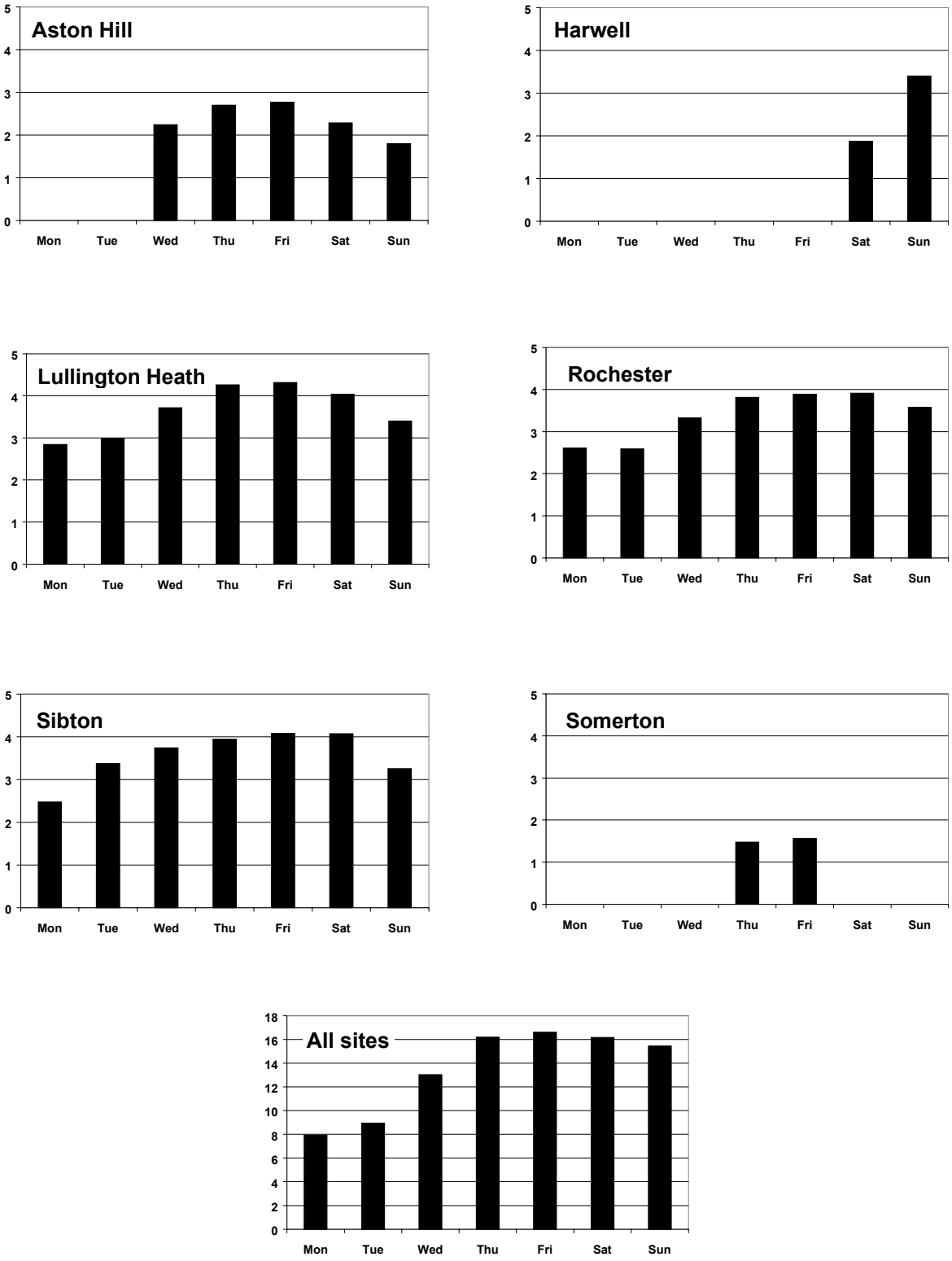

Figure 15: Variation of inferred number with hours ≥ 90 ppbv ozone with day of week at 6 southern UK sites, for the meteorological conditions of 31 July 1999.

of ozone episodes in the UK, it must be remembered that it is a case study which may not yield all the features which might be obtained if calculations were performed for a large number of events. In the present case, the calculated total figure for Sunday in Figure 15 is clearly greatly influenced by the individual contribution of Harwell and may therefore overestimate the relative probability of ozone exceedences on Sundays in general. It is difficult, however, to put forward an explanation for the observed Wednesday minimum within the context of the day of week emissions variation estimated in the present study.

4 Acknowledgements

The work presented in this report was funded by the Department of the Environment, Transport and the Regions (DETR) under contracts EPG 1/3/134 and 1/3/143. The present work would not have been possible without the groundwork of Dick Derwent (UK Meteorological Office) and Garry Hayman (AEA Technology) in the development and adaptation of the photochemical trajectory model, the contributions of Paul Willis and Trevor Davies (both AEA Technology) to the analysis of ozone exceedence data, and Sam Saunders (University of Leeds) to the testing of the CRI Mechanism.

5 References

Derwent R.G., M.E. Jenkin, S.M. Saunders and M.J. Pilling. (1998) Photochemical Ozone Creation Potentials for Organic Compounds in North West Europe Calculated with a Master Chemical Mechanism. Atmospheric Environment, 32, 2419-2441.

DUKES (1999). Department of Trade and Industry 'Digest of United Kingdom Energy Statistics 1999'. Government Statistical Sevice. Stationery Office, London.

Guenther A., Zimmerman P. and Wildermuth M. (1994). Natural volatile organic emission rate estimates for US woodland landscapes. Atmospheric Environment, 28, 1197-1210.

Hough A.M. (1988) The Calculation of Photolysis Rates for Use in Global Tropospheric Modelling Studies AERE Report R-13259, HMSO, London [ISBN 0-7058-1259-6].

Jenkin M.E., T.J. Davies, G.D. Hayman, J.R. Stedman, R. Thetford, P.L. Fitzgerald, R.G. Derwent, W.J. Collins, S.M. Saunders and M.J. Pilling (2000) Modelling of Tropospheric Ozone Formation. First annual report on the DETR contract EPG 1/3/143. Report AEAT/R/ENV/0099 Issue 1.

Passant N.R. and E. Lymberidi (1998) Emissions of non-methane volatile organic compounds from processes and solvent use. AEA Technology report AEAT-2837 Issue 1.

Simpson D., Guenther A., Hewitt C.N. and Steinbrecher R. (1995). Biogenic emissions in Europe: 1 Estimates and uncertainties. Journal of Geophysical Research, 100, 22875-22890.

UNECE (1991) Protocol to the 1979 Convention on long-range transboundary air pollution concerning the control of emissions of volatile organic compounds or their transboundary fluxes. ECEIEB.AIR/30. United Nations Economic Commission for Europe, Geneva, Switzerland

UNECE (1992) Air Pollution Studies 8: Impacts of Long-range Transboundary Air Pollution. Published by United Nations.

UNECE (1993) Air Pollution Studies 9: The State of Transboundary Air Pollution 1992 Update. Published by United Nations.

UNECE (1994) Environmental Conventions Published by United Nations.

Appendices

CONTENTS

Appendix 1

Trade associations contacted for information on the timing of members activities

Trade association

British Association of Chemical Specialities

British Coating Federation

British Wood Preservation and Damproofing Association

British Printing Industries Federation

British Sugar

European Coil Coating Federation

Film Coating Industry Group

Federation of Bakers

Metal Packaging Manufacturers Association

Made Up Textiles Association

Refined Bitumen Association

United Kingdom Petroleum Industries Association

Wallpaper Manufacturers Association

Appendix 2

Plots of 96-hour back trajectories to 8 southern UK rural sites, arriving at 1600 hr on Saturday 31 July 1999

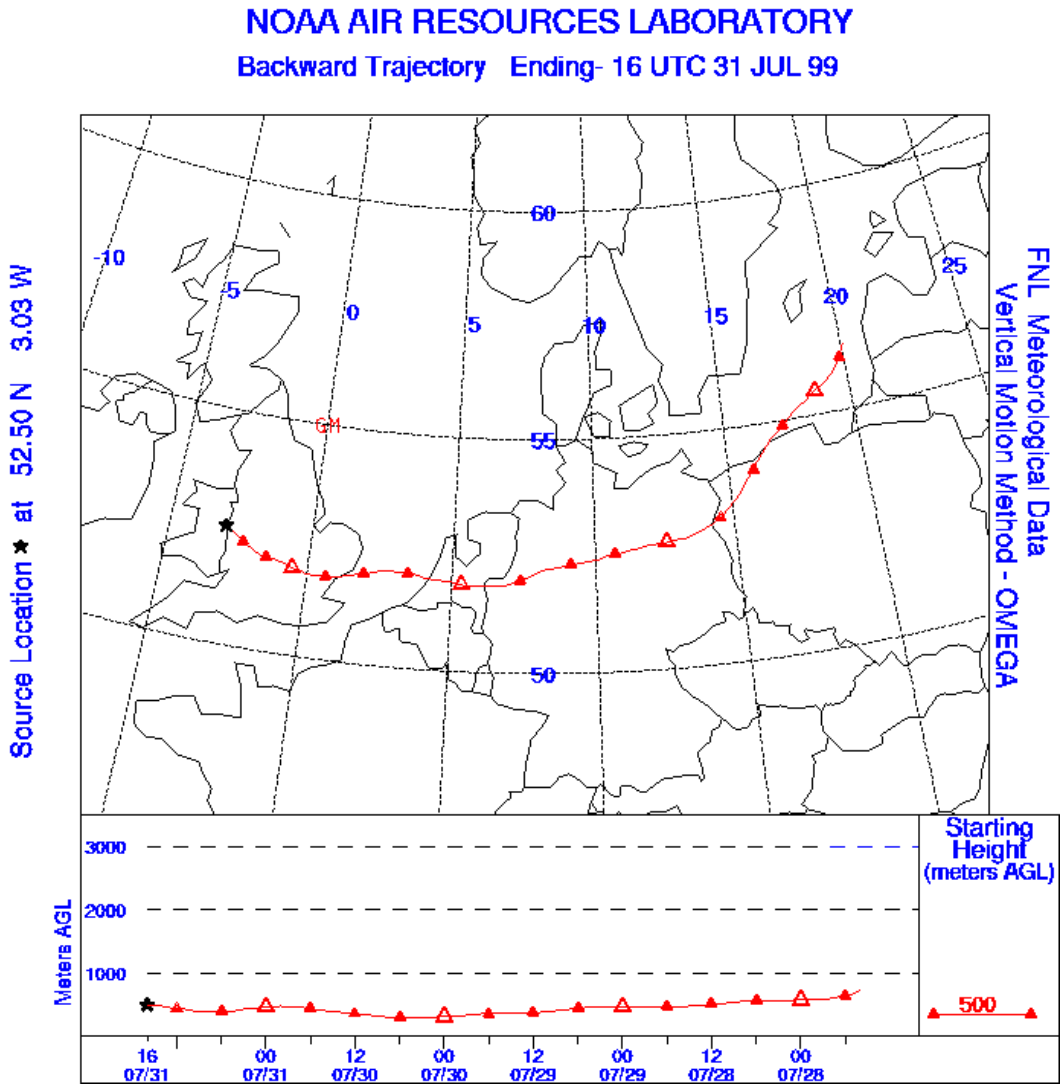

Figure A1.1: A plot of 96-hour back trajectory arriving at Aston Hill (Powys) at 1600 hr on Saturday 31 July 1999.

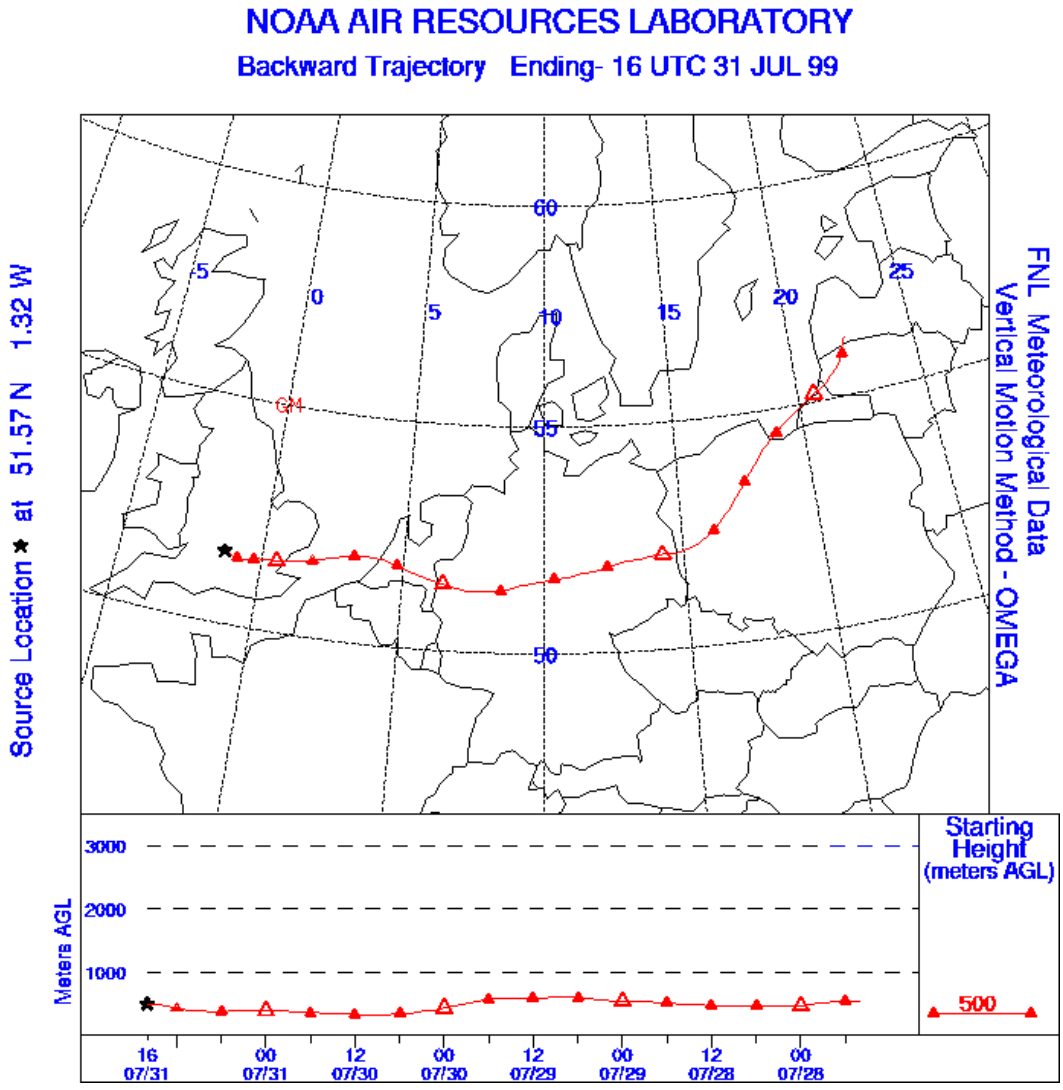

Figure A1.2: A plot of 96-hour back trajectory arriving at Harwell (Oxfordshire) at 1600 hr on Saturday 31 July 1999.

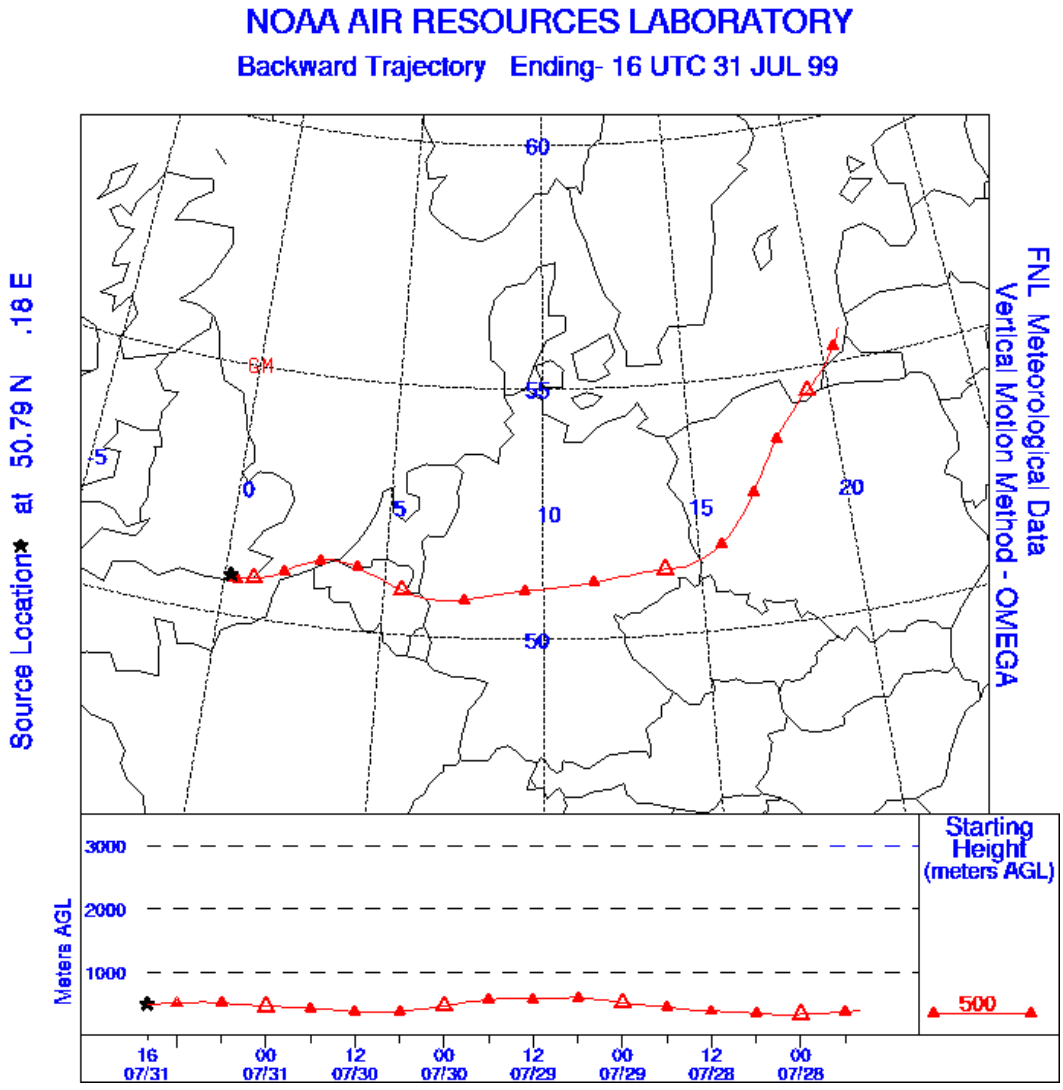

Figure A1.3: A plot of 96-hour back trajectory arriving at Lullington Heath (Sussex) at 1600 hr on Saturday 31 July 1999.

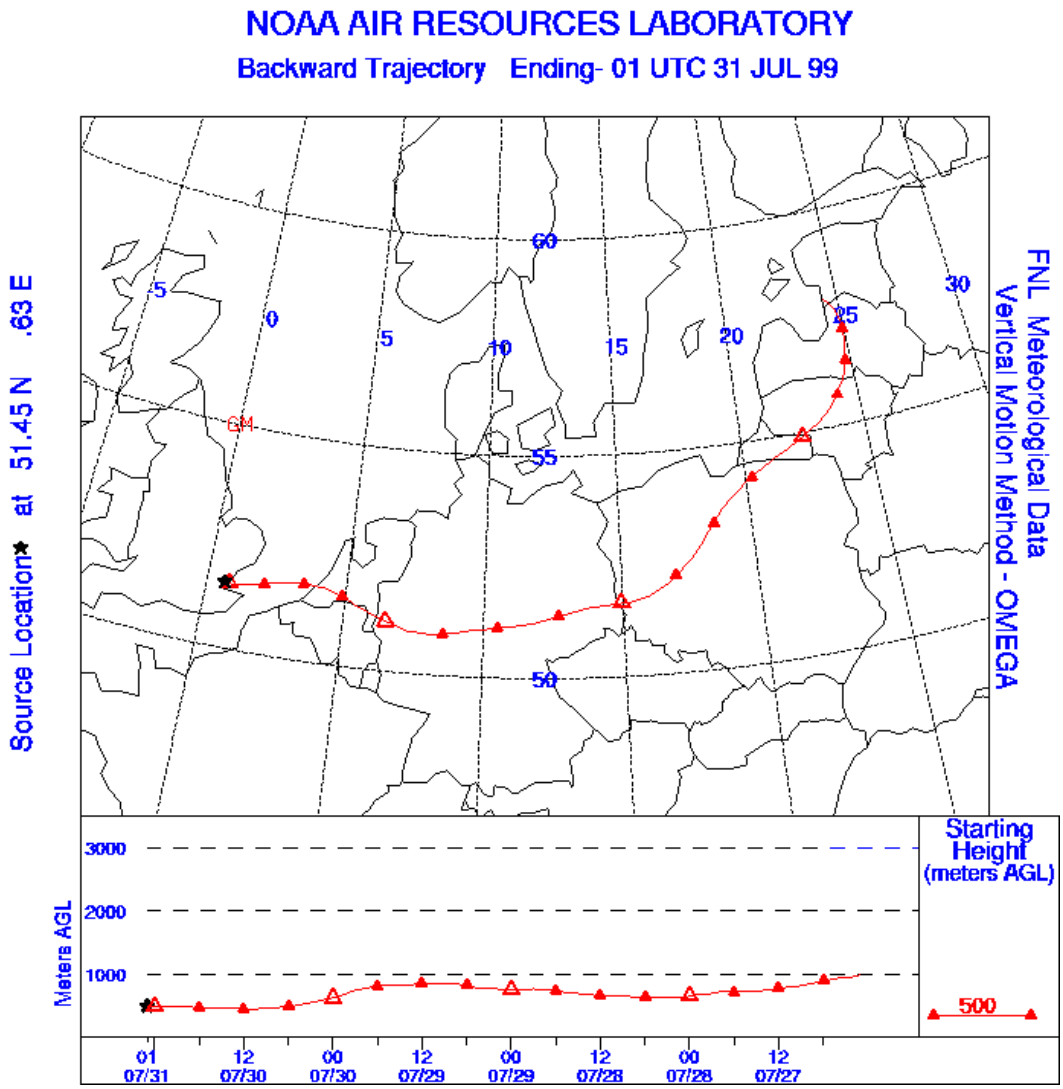

Figure A1.4: A plot of 96-hour back trajectory arriving at Rochester (Kent) at 1600 hr on Saturday 31 July 1999.

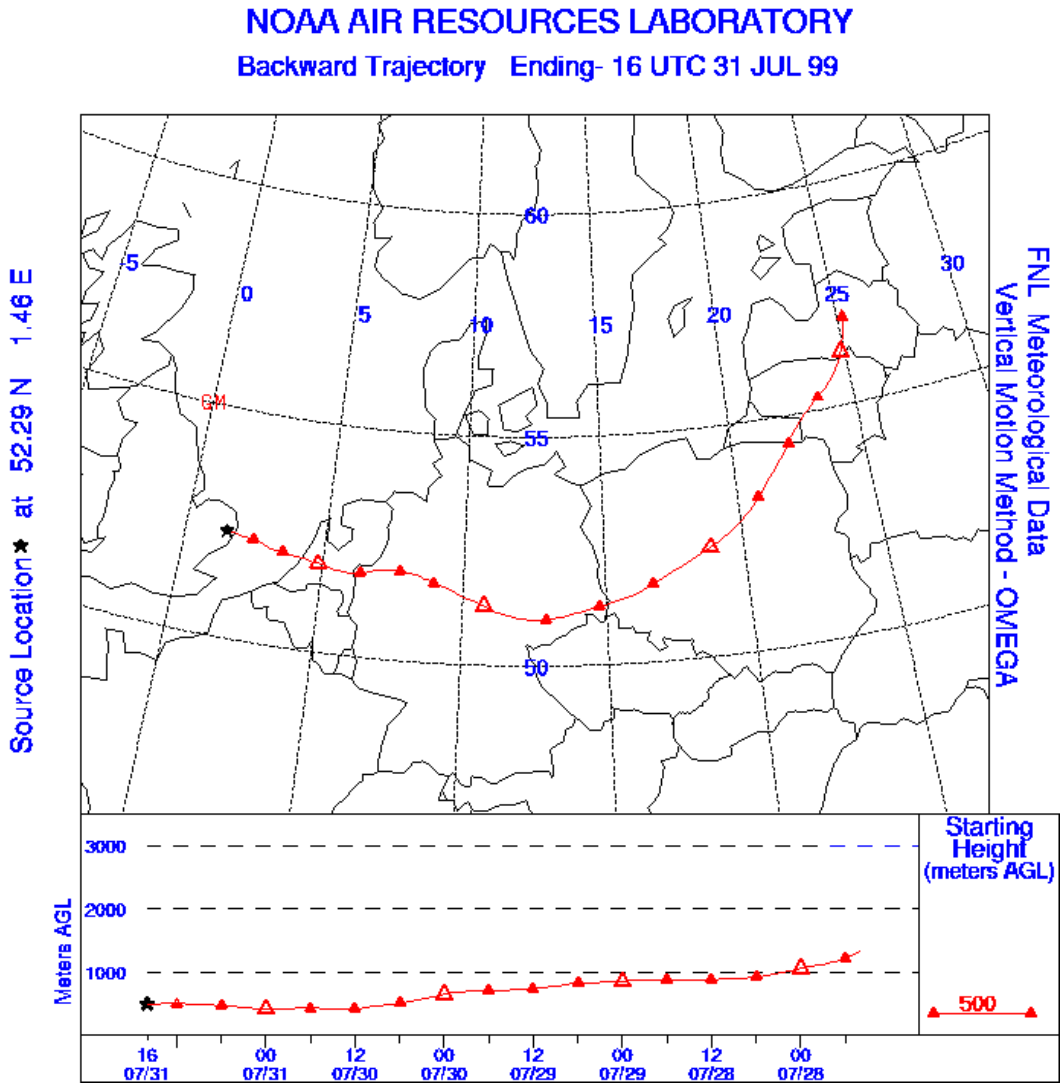

Figure A1.5: A plot of 96-hour back trajectory arriving at Sibton (Suffolk) at 1600 hr on Saturday 31 July 1999.

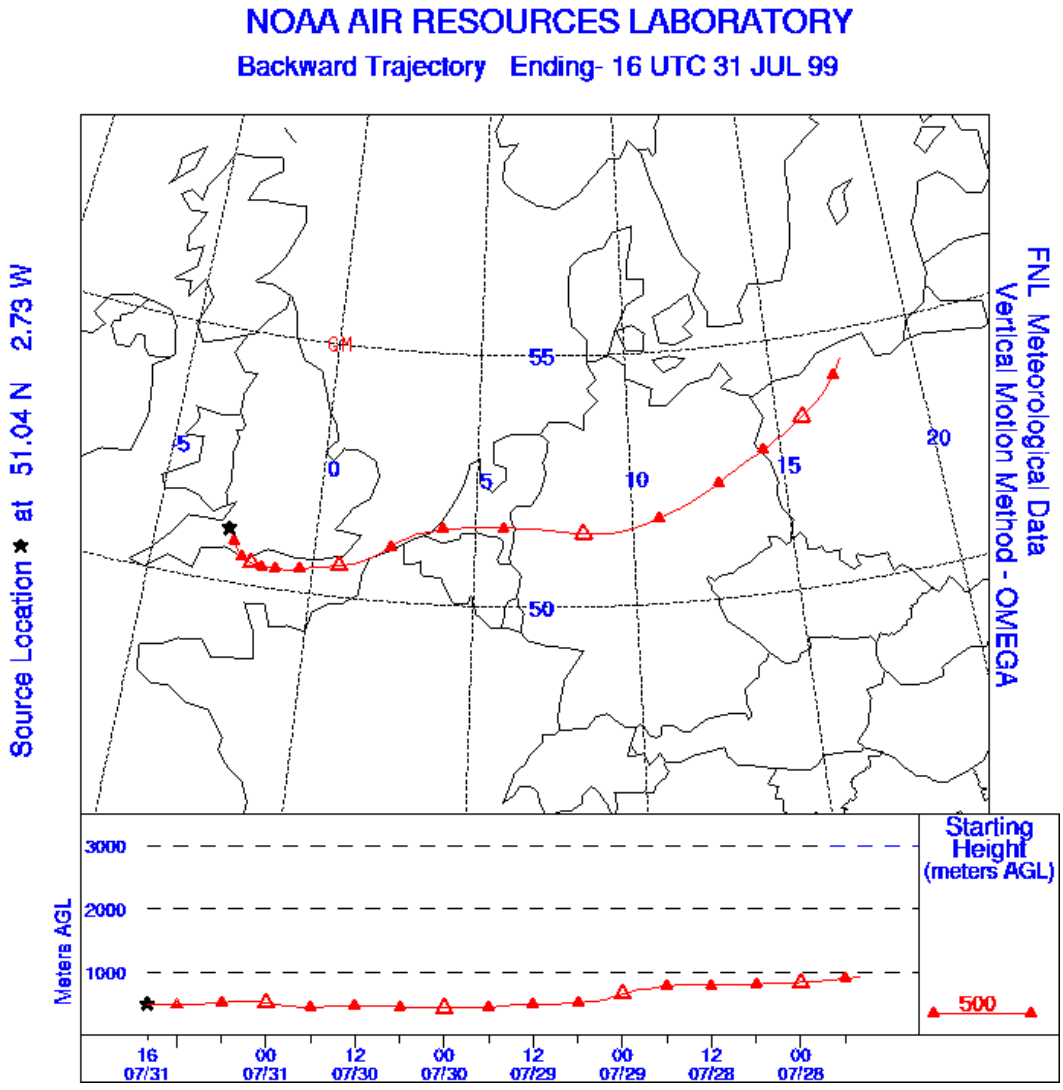

Figure A1.6: A plot of 96-hour back trajectory arriving at Somerton (Somerset) at 1600 hr on Saturday 31 July 1999.

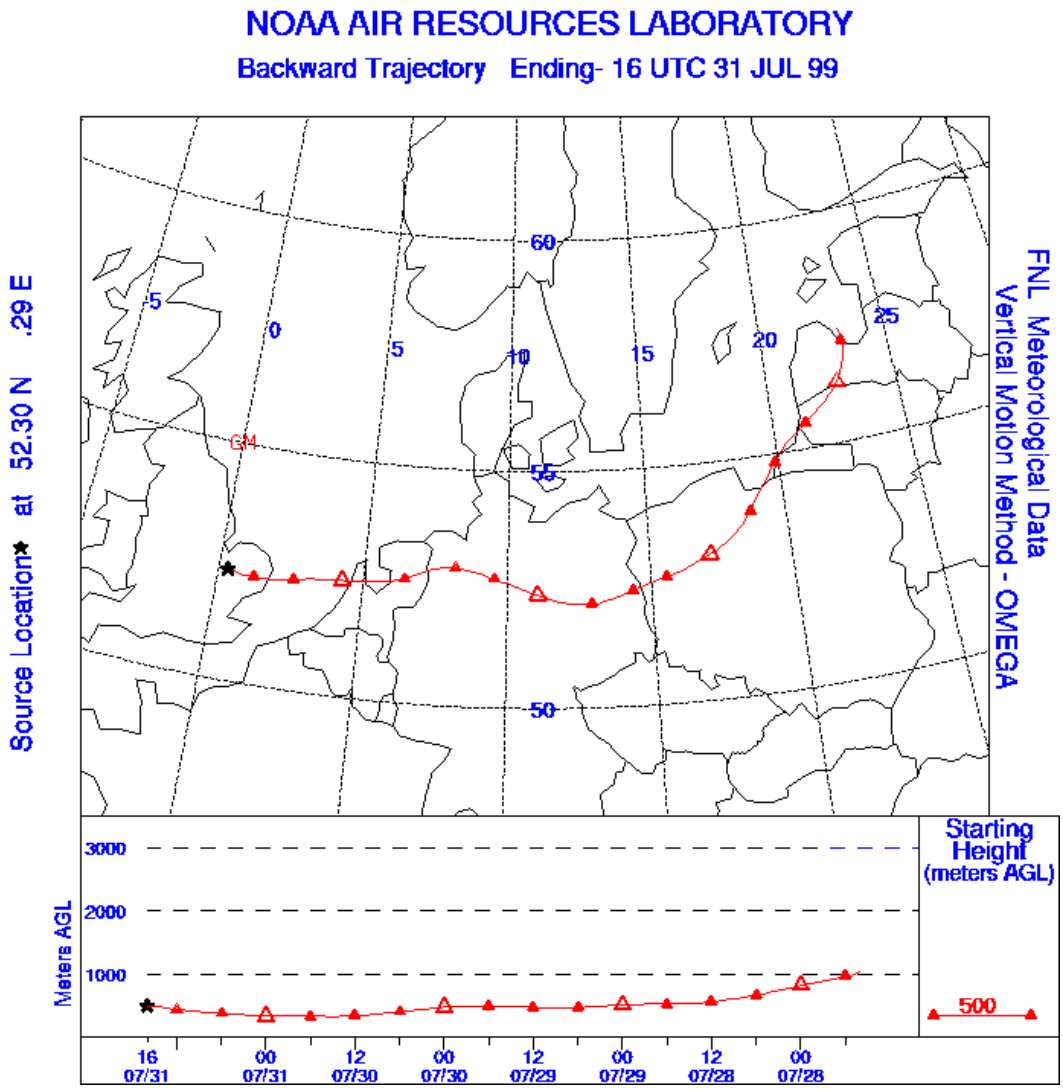

Figure A1.7: A plot of 96-hour back trajectory arriving at Wicken Fen (Cambridgeshire) at 1600 hr on Saturday 31 July 1999.

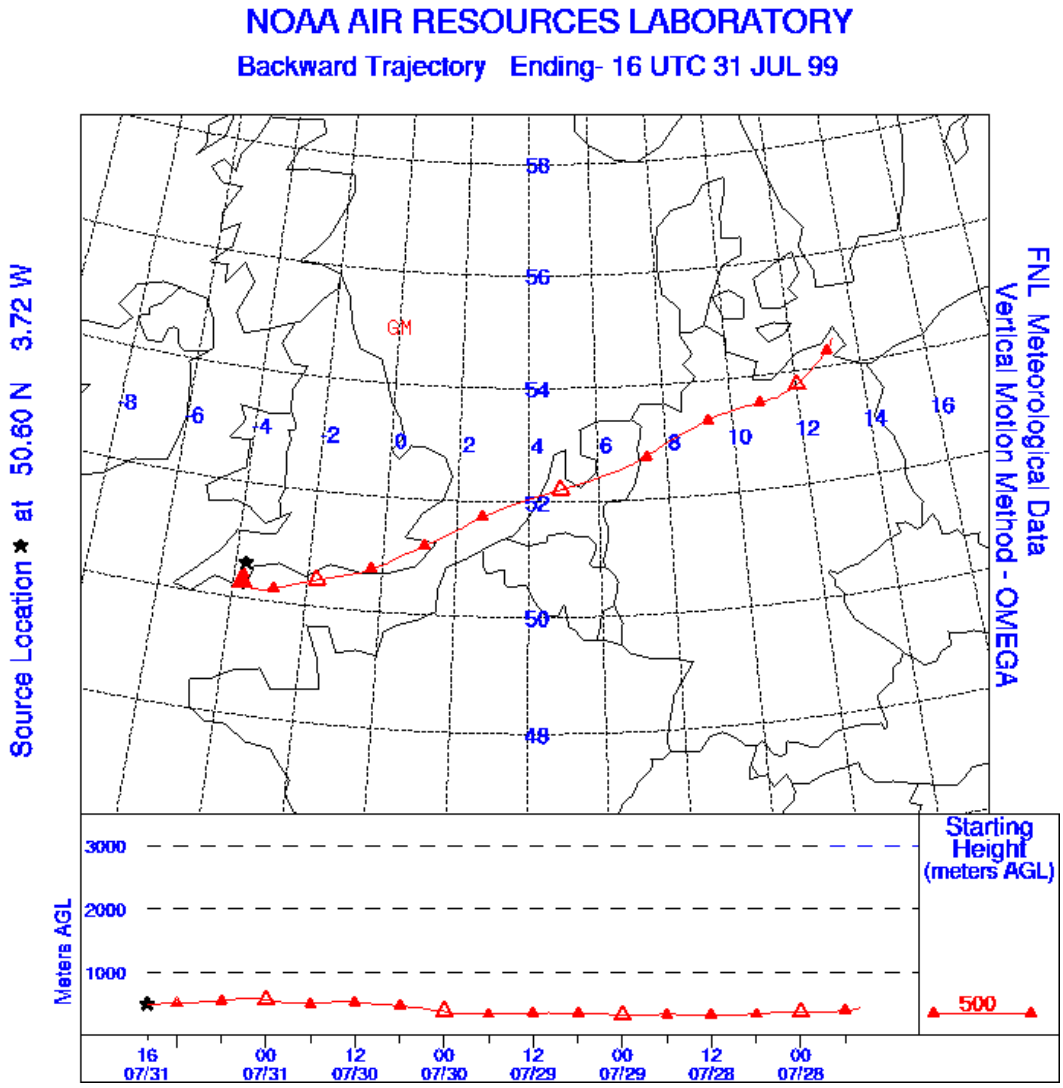

Figure A1.8: A plot of 96-hour back trajectory arriving at Yarner Wood (Devon) at 1600 hr on Saturday 31 July 1999.